The ER chaperone PfGRP170 is essential for asexual development and is linked to stress response in malaria parasites.

Heather M. Kudyba[1,2], David W. Cobb[1,2], Manuel A. Fierro[1,2], Anat Florentin[1], Dragan Ljolje[3], Balwan Singh[3], Naomi W. Lucchi[3], and Vasant Muralidharan[*,1,2]

[1]*Center for Tropical and Emerging Global Diseases, University of Georgia, Athens, Georgia, USA*

[2]*Department of Cellular Biology, University of Georgia, Athens, Georgia, USA*

[3]*Malaria Branch and Division of Parasitic Diseases and Malaria, Centers for Disease Control and Prevention, Atlanta, USA*

**Address correspondence to Vasant Muralidharan, vasant@uga.edu*

ABSTRACT

The vast majority of malaria mortality is attributed to one parasite species: *Plasmodium falciparum*. Asexual replication of the parasite within the red blood cell is responsible for the pathology of the disease. In *Plasmodium,* the endoplasmic reticulum (ER) is a central hub for protein folding and trafficking as well as stress response pathways. In this study, we tested the role of an uncharacterized ER protein, PfGRP170, in regulating these key functions by generating conditional mutants. Our data show that PfGRP170 localizes to the ER and is essential for asexual growth, specifically required for proper development of schizonts. PfGRP170 is essential for surviving heat shock, suggesting a critical role in cellular stress response. The data demonstrate that PfGRP170 interacts with the *Plasmodium* orthologue of the ER chaperone, BiP. Finally, we found that loss of PfGRP170 function leads to the activation of the *Plasmodium* eIF2α kinase, PK4, suggesting a specific role for this protein in this parasite stress response pathway.

INTRODUCTION

Malaria is a deadly parasitic disease that causes over 212 million cases and nearly 430,000 deaths each year, primarily in children under the age of five[1]. The deadliest human malaria parasite, *P. falciparum*, infects individuals inhabiting subtropical and tropical regions. These are some of the most impoverished regions of the world, making diagnosis and treatment challenging. Moreover, the parasite has evolved resistance to all clinically available drugs, highlighting an important need for uncovering proteins that are essential to the biology of this parasite[2-6]. Malaria is associated with a wide array of clinical symptoms, such as fever, chills, nausea, renal failure, pulmonary distress, cerebral malaria, and cardiac complications. It is the asexual replication of the parasite within the red blood cell (RBC) that is responsible for the pathology of the disease[7].

In *P. falciparum,* the endoplasmic reticulum (ER) is a uniquely complex, poorly understood organelle. In fact, recent data suggest that ER proteins play a major role in resistance to the frontline antimalarial, artemisinin[8-10]. It is in this organelle that a variety of essential cellular functions occur, including protein trafficking, cellular signaling, and activation of stress response pathways[11-17]. Compared to other eukaryotes, the molecular mechanisms involved in these essential processes in *Plasmodium* remain poorly understood. Therefore, it is imperative to uncover proteins that regulate and maintain ER biology. One group of proteins likely governing many of these processes are ER chaperones[18-23].Very little is known about the roles that ER chaperones play in *Plasmodium*, many of them defined merely based on sequence homology to other organisms. The *Plasmodium* genome encodes a relatively reduced repertoire of predicted ER chaperones, but it is predicted to contain two members of the conserved ER HSP70 chaperone complex, GRP78 (or BiP) and a putative HSP110 (PfGRP170 or PfHSP70-y)[24,25]. GRP170, in other eukaryotes, serves as nucleotide exchange factor for BiP[26,27]. Additionally, GRP170 has been reported to have holdase activity and can bind unfolded substrates independent of ATP or BiP[28-30].

In this study, we used a conditional auto-inhibition strategy to generate conditional mutants for the putative ER chaperone, PfGRP170 (PF3D7_1344200)[31-33]. Using these

59 conditional mutants, we localized PfGRP170 to the parasite ER, and show that unlike its
60 orthologs in other eukaryotes, PfGRP170 is essential for parasite survival. Detailed life
61 cycle analysis revealed that inhibition of PfGRP170 results in parasite death in early
62 schizogony. The protein is required for surviving a brief heat shock, suggesting that
63 PfGRP170 is essential during febrile episodes in the host. We show that despite a
64 predicted transit peptide, PfGRP170 is not essential for protein trafficking to the
65 apicoplast. Trafficking experiments using antibodies for two PEXEL Negative Exported
66 Proteins and one protein containing a Plasmodium Export Element indicates that
67 PfGRP170 is unlikely to be involved in protein export. Using a combination of mass
68 spectroscopy approaches we identified potential interactors. Moreover, we demonstrate
69 here that PfGRP170 interacts with the *Plasmodium* homolog of BiP (PF3D7_0917900)
70 suggesting a conserved HSP70 ER chaperone complex. Finally, we show that conditional
71 inhibition of PfGRP170 leads to the activation of the only known ER stress response
72 pathway in Plasmodium, the PK4 pathway[10,16].
73
74 **RESULTS**
75 ***PF3D7_1344200 is a putative GRP170 in P. falciparum***
76 A blast search to identify ER localized Hsp70 proteins in *P. falciparum* revealed two
77 proteins, HSP70-2 (PfGRP78/BiP) and a putative HSP110 (PF3D7_1344200). HSP110
78 proteins are considered large HSP70 chaperones, having sequence homology to both
79 the nucleotide and substrate binding domains of other HSP70 members[34]. The increased
80 size of HSP110 family members is the result of an extended α-helical domain at the C-
81 terminus as well as an unstructured loop inserted in the substrate-binding domain[28,34]
82 (Figure 1A). In other eukaryotic organisms, the ER localized HSP110 (referred to as
83 GRP170) is a chaperone with four primary protein domains: a signal peptide, a nucleotide
84 binding domain, a substrate binding domain, and an extended C-terminus[26,34]. A protein
85 sequence alignment using the yeast GRP170 (Lhs1) was used to predict the boundaries
86 of these domains in PF3D7_1344200 (PfGRP170) (Figure 1A and Supplemental Figure
87 1). Most of the sequence conservation between Lhs1 and PfGRP170 was found to be in
88 the nucleotide binding domain (Supplemental Figure 1). PfGRP170 is well conserved
89 across multiple *Plasmodium* species, including other human malaria-causing species

90 (Supplemental Figure 2). This level of conservation decreases in another apicomplexan
91 (*T. gondii*) and even more so in yeast and humans (Supplemental Figure 2).
92
93 ***Generating PfGRP170-GFP-DDD conditional mutants***
94 Conditional mutants for PfGRP170 (termed PfGRP170-GFP-DDD) were generated by
95 tagging the endogenous PfGRP170 locus at the 3' end, using single homologous
96 crossover, with a GFP reporter, the *E. coli* DHFR destabilization domain (DDD), and an
97 ER retention signal (SDEL) (Figure 1B). The endogenous PfGRP170 gene encodes a C-
98 terminus SDEL sequence, a potential ER retention signal, and therefore we added an
99 SDEL sequence after the DDD domain in order to avoid mislocalization of the tagged
100 protein. In the presence of the small ligand Trimethoprim (TMP), the DDD is maintained
101 in a folded state. However, if TMP is removed from the culture medium, the DDD unfolds
102 and becomes unstable[31-33,35,36]. Intramolecular binding of the chaperone to the unfolded
103 domain inhibits normal chaperone function (Figure 1B)[31-33]. Two independent
104 transfections were carried out, and integrated parasites were selected via several rounds
105 of drug cycling. PCR integration tests following drug selection indicated that the
106 percentage of integrated parasites in both transfections were extremely low (Figure 1C).
107 Consequently, standard limiting dilution could not be used to clone out integrated
108 parasites. To circumvent this issue, flow cytometry was used to enrich and sort extremely
109 rare GFP positive parasites. Despite low enrichments and sorting rates (GFP positive
110 population =~1.13E-3), we successfully obtained two clones, termed 1B2 and 1B11, using
111 flow sorting (Figure 1 C and D). Proper integration into the *pfgrp170* locus was confirmed
112 by a Southern blot analysis (Figure 1E). Western blot analysis revealed that the
113 PfGRP170-GFP-DDD protein was expressed at the expected size (Figure 1F).
114 Immunofluorescence assays (IFA) and western blot analysis showed that the PfGRP170-
115 GFP-DDD fusion protein was expressed and localized to the parasite ER during all stages
116 of the asexual life cycle (Figure 1G and Supplemental Figure 3).
117
118 ***PfGRP170 is essential for asexual growth and surviving febrile episodes***
119 To investigate the essentiality of PfGRP170, PfGRP170-GFP-DDD asynchronous
120 parasites were cultured in the absence of TMP, and parasitemia was observed using flow

121 cytometry. A growth defect was seen within 24 hours after the removal of TMP, resulting
122 in parasite death (Figure 2A). Furthermore, the two clonal parasite lines exhibited a dose-
123 dependent growth response to TMP (Figure 2B). Consistent with data from other
124 chaperones tagged with the DDD[31-33], TMP removal did not result in degradation of
125 PfGRP170-GFP-DDD (Figure 2C). Conditional inhibition of *Plasmodium* proteins that
126 does not involve their degradation, has also been observed for other non-chaperone
127 proteins [37,38]. Moreover, the removal of TMP did not affect the ER localization of
128 PfGRP170 (Supplemental Figure 4).
129
130 Using a nucleic acid stain, acridine orange, we used flow cytometry to specifically observe
131 each stage of the asexual life cycle (ring, trophozoite, and schizont) in PfGRP170-GFP-
132 DDD parasites incubated with and without TMP (Figure 2D). The amounts of RNA and
133 DNA increase over the asexual life cycle as the parasite transitions from a ring to
134 trophozoite to a multi-nucleated schizont. We observed that upon TMP removal, mutant
135 parasites arrested in a relatively late developmental stage (Figure 2D). To identify the
136 stage in the asexual life cycle where the mutant parasites died, TMP was removed from
137 tightly synchronized ring stage cultures and parasite growth and morphology was
138 assessed over the 48-hour life cycle. We observed morphologically abnormal parasites
139 late in the lifecycle, when control parasites had undergone schizogony (Figure 2E). The
140 PfGRP170-GFP-DDD parasites grown without TMP ultimately failed to progress through
141 schizogony and did not reinvade new RBCs (Figure 2E).
142
143 The cytoplasmic ortholog of PfGRP170, PfHSP110, was previously shown to be essential
144 for surviving heat stress[33]. Therefore, we tested whether PfGRP170 mutants were
145 sensitive to a brief heat shock. Asynchronous parasites were incubated in the absence of
146 TMP for 6 hours at either 37°C or 40°C. Following the 6-hour incubation, TMP was added
147 back to all cultures, which were then grown at 37°C for two growth cycles, while
148 measuring parasitemia every 24 hours. The growth of parasites at 37°C was not
149 significantly affected by the brief removal of TMP (Figure 2F). In contrast, incubating
150 parasites at 40°C without TMP resulted in reduced parasite viability compared to
151 parasites grown at 40°C with TMP (Figure 2F).

152

153 ***PfGRP170 is not required for trafficking of apicoplast proteins***

154 Protein trafficking to the apicoplast is essential for parasite survival. Proteins targeted to
155 the apicoplast contain an N-terminal transit peptide that is revealed upon signal peptide
156 cleavage in the ER[15,39]. It remains unclear whether apicoplast targeted proteins go
157 through the Golgi before reaching their final destination. It has been shown that disruption
158 of ER to Golgi trafficking, using Brefeldin A (BFA), does not reduce apicoplast
159 transport[15,40]. One of these studies further demonstrated that the addition of an ER
160 retention sequence (SDEL), to a GFP with a transit peptide, did not reduce apicoplast
161 trafficking or transit peptide cleavage[40]. However, a separate but similar analysis came to
162 the opposite conclusion[41]. Thus, the identification, packaging, and transport of apicoplast-
163 targeted proteins from the ER remain unanswered questions.

164

165 Two software analysis tools (Prediction of Apicoplast-Targeted Sequences (PATS) and
166 PlasmoAP) predicted a strong apicoplast transit peptide for PfGRP170, despite our
167 observation of a definite ER localization (Figure 1G and Figure 3A). We were therefore
168 interested to find out whether PfGRP170 plays a role in apicoplast trafficking. We tested
169 whether the putative PfGRP170 transit peptide (amino acids: 1 to 150) could be trafficked
170 to the apicoplast by episomally expressing the predicted PfGRP170-transit peptide fused
171 to a GFP reporter without an ER retention signal (Figure 3B). We performed co-
172 localization assays using ER, apicoplast, and Golgi markers and determined that the
173 putative transit peptide localized to the ER due to colocalization with ER marker
174 Plasmepsin V (Figure 3B).

175 To determine the role of PfGRP170 in trafficking proteins to the apicoplast, we removed
176 TMP from PfGRP170-GFP-DDD parasites and examined the localization of the
177 apicoplast-localized cpn60[32,42,43]. No defects in apicoplast localization of cpn60 were
178 observed (Figure 3C). Additionally, incubation with the essential apicoplast metabolite
179 IPP[44], failed to rescue or have any positive effect on TMP removal in PfGRP170-GFP-
180 DDD parasites (Figure 3D).

181

182 ***Interactions of PfGRP170***

183 Two independent approaches were taken to identify the interacting proteins of PfGRP170
184 (Figure 4A). The first was an anti-GFP Immunoprecipitation (IP) followed by mass
185 spectroscopy. In the second approach we generated a parasite line episomally
186 expressing PfGRP170 tagged with an HA, the promiscuous Biotin Ligase (BirA), and an
187 ER retention signal (KDEL). When exogenous biotin is added to the PfGRP170-HA-BirA
188 parasites, the BirA tagged protein will biotinylate interacting proteins or those that are in
189 close proximity[45]. These biotinylated proteins were isolated using streptavidin coated
190 magnetic beads. A western blot analysis confirmed expression of the PfGRP170-HA-BirA
191 fusion protein (Supplemental Figure 5A). Colocalization IFA's confirmed that the
192 PfGRP170-HA-BirA protein localizes to the parasite ER (Supplemental Figure 5B).
193 Additionally, western blot analysis demonstrates that proteins are biotinylated in the
194 PfGRP170-HA-BirA parasite lines when biotin is added (Supplemental Figure 5C).
195

196 Mass spectroscopy was used to identify PfGRP170 interacting proteins from two
197 independent anti-GFP IP's of PfGRP170-GFP-DDD parasites and two biological
198 replicates of streptavidin pulldowns from PfGRP170-HA-BirA parasites following an
199 incubation with biotin (Supplemental Table 1). Further, two independent anti-GFP IP's
200 from the PM1 parental control and one streptavidin pull down from 3D7 parasites
201 incubated with biotin to filter out non-specific interactions (Supplemental Table 1). Both
202 BiP and PfGRP170 were found in the control IP's, albeit in lower peptide counts
203 (Supplemental Table 1). This is not surprising as chaperones are common contaminants
204 in mass spectroscopy. However, due to the documentation of PfGRP170 being an
205 interactor and regulator of BiP function, we opted to keep BiP in our analysis[26]. In order
206 to obtain a list of proteins specific to the ER and parasite secretory pathway, proteins
207 identified by mass spectroscopy in each IP were filtered to include only those, which had
208 a signal peptide or transmembrane domain. Thirty proteins were found in both the 1B2
209 and 1B11 in the anti-GFP IP's and 37 proteins were found in the two replicates of the
210 PfGRP170-HA-BirA streptavidin pull down (Figure 4A). Of these, 11 proteins were
211 identified using both approaches suggesting that these are true interactors of PfGRP170
212 (Figure 4B). Using recently published real-time transcriptional abundance data, we plotted

213 the normalized transcriptional abundance values for all 11 proteins[46] (Supplemental
214 Figure 6). Upon removal TMP, the PfGRP170-DDD parasites die 38-44 hours post
215 invasion (Figure 2E) and therefore, it is likely that the essential function of PfGRP170 is
216 linked to proteins expressed during these late stages of the asexual life-cycle. Excluding
217 proteins which were expressed earlier in the life cycle, narrows the list of putative
218 essential interactors of PfGRP170 to the seven proteins (Figure 4C)[46].

219 ***PfGRP170 is not required for trafficking to the RBC***

220 In order for the parasite to grow, develop, and divide, it must drastically remodel the host
221 RBC[12]. These modifications are accomplished through the export of proteins from the ER
222 to the RBC. In model eukaryotes, such as yeast and mammalian cells, molecular
223 chaperones, and specifically those that are ER-localized, play central roles in protein
224 trafficking[18,19]. Therefore, we tested whether conditional inhibition of PfGRP170 would
225 prevent trafficking of several exported proteins (PfHSP70x, PfMAHRP1, and FIKK4.2).
226 Our results demonstrate that loss of PfGRP170 function did not affect the localization of
227 these proteins to the host RBC (Supplemental Figure 7A-C).
228

229 ***PfGRP170 and BiP interact***

230 One of the most abundant proteins identified in our mass spectroscopy data was PfBiP
231 (Figure 4B and Supplemental Table 1). However, PfBiP was also found in our IPs
232 performed with parental controls, therefore, we were tested whether PfGRP170 and PfBiP
233 interact in *P. falciparum*. We performed an anti-GFP Co-IP and probed the lysate for
234 PfBiP. We observed that PfGRP170 and PfBiP interact and this interaction is not lost
235 upon TMP removal (Figure 5A). As a control, we probed the GFP Co-IP lysates for a
236 different ER protein, Plasmepsin V (PMV), and found that it did not pull down with
237 PfGRP170 (Figure 5B).
238

239 To visualize the PfGRP170-PfBiP interaction within the cellular context of the infected
240 RBC, we utilized a Proximity Ligation Assay (PLA)[47-49]. The PLA positive signal indicates
241 that two proteins are within 40nm of each other, suggesting a close interaction within the
242 cell. This approach has been used successfully in *Plasmodium* to demonstrate interaction
243 of exported proteins[50]. We performed this assay using anti-GFP and anti-BiP antibodies

244 and observed a positive signal at all life cycle stages (Figure 5C). As a negative control
245 we also probed with an antibody against the ER localized protease PMV and despite the
246 co-localization of these two proteins in the ER, we did not see a positive PLA signal,
247 suggesting distinct sub-organellar localizations (Figure 5D). Together, these results
248 demonstrate that PfGRP170 and PfBiP interact during all stages of the asexual life cycle
249 of *P. falciparum.*
250
251 The function of BiP is critical for ER biology and in other eukaryotes its function is
252 regulated by GRP170[26,27]. Additionally, loss of the PfGRP170 yeast homolog, Lhs1,
253 activates a stress response mechanism known to upregulate BiP expression[51]. Therefore,
254 we tested whether the PfGRP170-GFP-DDD mutants could be rescued by
255 overexpression of PfBiP. We did this by episomally expressing PfBiP with a Ty1 tag and
256 an ER retention signal (KDEL) in the PfGRP170-GFP-DDD mutants. Colocalization
257 assays demonstrate that the PfBiP-Ty1 fusion protein is targeted to the ER and we
258 observe that the protein is expressed at the expected size by western blot (Figure 5E and
259 5F). To determine if the overexpression of PfBiP could rescue parasite growth during
260 TMP removal, the PfGRP170-GFP-DDD parasites expressing the PfBiP-Ty1 protein were
261 incubated with and without TMP and the parasitemia was monitored using flow cytometry.
262 We demonstrate that the overexpression of PfBiP in the PfGRP170-GFP-DDD parasites
263 could not rescue parasite growth (Figure 5G).
264
265 ***Loss of PfGRP170 function activates the PK4 stress response pathway***
266 In addition to their function in the secretory pathway, molecular chaperones perform a
267 vital role in the management of cellular stress. *Plasmodium* lack much of the ER
268 machinery used to activate stress response pathways[16,52,53]. The only identified ER stress
269 response pathway in *Plasmodium* is the PERK/PK4 pathway[10,16]. Signaling through this
270 pathway has been shown to occur in the parasite following artemisinin treatment[10]. Under
271 normal conditions, PK4 exists as a transmembrane monomeric protein in the ER. When
272 the ER is stressed, PK4 oligomerizes and becomes active, phosphorylating the
273 cytoplasmic translation initiation factor EIF2-α to halt translation and flux through the
274 ER[10,16]. To determine whether this pathway was activated during conditional inhibition of

275 PfGRP170, PfGRP170-GFP-DDD parasites were tightly synchronized to the ring stage
276 and grown without TMP for 24 hours, after which parasite lysate was collected and the
277 phosphorylation state of EIF2-α determined by western blot. We observed that PfGRP170
278 auto-inhibition resulted in the phosphorylation of EIF2-α, indicating that this pathway was
279 activated (Figure 6A).
280
281 Since conditional inhibition of PfGRP170 resulted in EIF2-α phosphorylation, which has
282 been shown to be required for resistance to artemisinin resistance, we tested if PfGRP170
283 plays a role in drug resistance. For this purpose, we utilized PfGRP170-BirA parasites,
284 which have an extra copy of PfGRP170. Using the ring-stage survival assay, we
285 compared the growth of the parental parasite line (3D7) with that of PfGRP170-BirA
286 parasites after brief exposure to artemisinin. Our data show that overexpression of
287 PfGRP170 did not result in artemisinin resistance (Supplemental Figure's 8A-B).
288
289 Several *Plasmodium* kinases have been shown to phosphorylate EIF2-α in late
290 developmental stages or in response to other cellular stress or artemisinin treatment[16,54-
291 56]. We were therefore interested in identifying the specific kinase that is responsible for
292 the phosphorylation of EIF2-α during conditional inhibition of PfGRP170. The ER kinase,
293 PK4, has been shown to be activated by ER stress in *Plasmodiu*m[53]. Therefore, we
294 incubated synchronized PfGRP170-GFP-DDD parasites without TMP for 24 hours, in the
295 presence or absence of a specific PK4 inhibitor GSK2606414[10]. Parasite lysates were
296 used to determine the phosphorylation state of EIF2-α. We observed that in the presence
297 of the PK4 inhibitor, EIF2-α phosphorylation was blocked, demonstrating that conditional
298 inhibition of PfGRP170 specifically results in PK4 activation, which leads to
299 phosphorylation of EF2-α (Figure 6B). As a control, we used the parental strain, PM1,
300 and incubated these parasites with and without TMP or the PK4 inhibitor (Supplemental
301 Figure 9). This experiment showed no changes in levels of EIF2-α regardless of the
302 presence of TMP or the PK4 inhibitor.
303
304
305

306 **DISCUSSION**

307 We present in this work the first characterization of PfGRP170 in the asexual life cycle of
308 *P. falciparum*. We have generated conditional mutants that allow us to probe the role of
309 this protein using the DDD conditional auto-inhibition system[32,33,35-38]. Additionally, taking
310 advantage of the GFP fused to PfGRP170, we were able to isolate an exceptionally rare
311 clonal population using flow cytometry. This technique achieved what a traditional limiting
312 dilution method could not. Moreover, this type of flow sorting can be implemented not only
313 for rare events but also to significantly cut down the time from transfection to a clonal cell
314 population.

315

316 We demonstrate here that PfGRP170 is an ER resident protein that is essential for
317 asexual growth in *P. falciparum*. Loss of PfGRP170 function leads to a growth arrest of
318 parasites late in development and their subsequent death. In yeast and mammals,
319 GRP170 functions in a complex with the ER chaperone BiP, serving as the nucleotide
320 exchange factor to regulate BiP activity[26,27]. Unlike *Plasmodium falciparum*, Yeast null for
321 GRP170 are viable due to the upregulation of Sil1, another nucleotide exchange factor,
322 that usually plays a role in the IRE1 stress response pathway[51]. The *Plasmodium* genome
323 does not encode Sil1 and IRE1, which aligns with the observed essentiality of PfGRP170
324 during the blood stages. Additionally, research in mammalian systems suggests that
325 GRP170 also has BiP-independent functions, such as binding unfolded substrates[28]. Our
326 data show, via immunoprecipitation, mass spectroscopy, and proximity ligation assays,
327 that PfGRP170 interacts with BiP in *P. falciparum* suggesting that it regulates BiP
328 function. Further, overexpression of PfBiP was unable to rescue loss of PfGRP170
329 function and the conditional inhibition of PfGRP170 does not reduce its interaction with
330 PfBiP. These data suggest that a PfBiP independent function of PfGRP170 is essential
331 for parasite survival.

332

333 Previously it was shown that apicoplast transit peptides are predicted to bind the ER
334 chaperone BiP, and when these predicted binding sites were mutated, targeting to the
335 apicoplast was disrupted[57]. Moreover, an Hsp70 inhibitor with an antimalarial activity was
336 shown to inhibit apicoplast targeting[58,59]. These data, combined with the predicted transit

337 peptide of PfGRP170, led us to investigate the role of this chaperone in apicoplast
338 trafficking. Interestingly, when the putative transit peptide was tagged with a GFP reporter
339 and without an ER retention signal, the fusion protein was retained in the ER. It was
340 previously reported that proteins with a signal peptide and no ER retention signal are
341 secreted to the parasitophorous vacuole[60-63]. However, it was also shown that some
342 proteins with a signal peptide and GFP (lacking an ER retention or trafficking signals)
343 remain in the parasite ER[61]. Regardless, this reporter was not sent to the apicoplast
344 indicating that it is not a functional apicoplast transit peptide. Previous work suggest that
345 appending the first 137 amino acids of PfGRP170 to a GFP reporter (without a retention
346 signal) resulted in this chimeric protein localizing partially to the apicoplast and to the
347 parasitophorous vacuole[64]. Our chimeric protein includes the first 150 amino acids of
348 PfGRP170 which may account for some of the differences in the two studies. In addition,
349 PfGRP170 auto-inhibition did not lead to any defects in trafficking to the apicoplast, nor
350 could it be rescued with the essential apicoplast metabolite IPP. Further, we did not
351 identify any apicoplast localized proteins as potential interactors of PfGRP170 These data
352 suggest that the primary function of PfGRP170 does not function in the apicoplast
353 trafficking pathway.
354
355 Protein trafficking to the host RBC originates in the parasite ER and is essential for
356 parasite viability, and therefore could potentially account for the observed death
357 phenotype during conditional inhibition of PfGRP170[11,12]. PfGRP170 was shown to
358 associate with exported proteins in another study that identified proteins that bind to the
359 antigenic variant surface protein, PfEMP1[65]. However, our data show that there is no
360 significant difference in the trafficking of some exported proteins upon conditional
361 inhibition of PfGRP170, suggesting that protein export is not blocked.
362
363 ER chaperones are known in other eukaryotes to be vital to managing cellular stress[17,21].
364 However, several ER localized stress response pathways present in other eukaryotes are
365 absent in *P. falciparum* and few molecular players in the parasite ER stress response
366 pathway are known. Our data demonstrate that PfGRP170 is important for coping with a
367 specific form of cellular stress, namely heat shock. This finding highlights a potential

368 critical role for PfGRP170 *in vivo*, as high febrile episodes are one of the main symptoms
369 of clinical malaria and are considered a defense mechanism against parasites. GRP170
370 in mammalian systems has been shown to bind to the transmembrane proteins in the ER
371 that are involved in the unfolded protein response (UPR), suggesting it may regulate
372 these pathways[66,67]. The *Plasmodium* genome does not encode many of the UPR
373 orthologues, but a single ER stress pathway (PK4 signaling) has been previously
374 described and was shown to be activated following artemisinin treatment[10,16]. Here, we
375 demonstrate that loss of PfGRP170 function results in the activation of PK4 stress
376 pathway, providing the first link between an endogenous ER resident protein and the
377 activation of the PK4 pathway in *P. falciparum*. Further, our data suggest that even though
378 the PK4 stress response pathway is activated upon removal of TMP, this pathway is
379 ultimately unable to prevent parasite death. This is most likely because one or more
380 essential proteins that depend of PfGRP170 for their correct folding and function.
381
382 Yeast null for the GRP170 homolog, Lhs1, activate the IRE1 UPR signaling pathway[51].
383 Activation of the IRE1 pathway in eukaryotes, which is not present in *Plasmodium,*
384 typically leads to the upregulation of ER chaperones such as BiP[51-53,68]. These data
385 suggest that the only essential function of Lhs1 is to serve as a nucleotide exchange
386 factor for BiP[51]. Therefore, we tested whether the death phenotype seen in the conditional
387 PfGRP170 mutants could be rescued by overexpressing PfBiP. Our experiments
388 revealed that overexpression of PfBiP does not improve viability of the PfGRP170-GFP-
389 DDD parasites following TMP removal. This data implies, that unlike its homologs in other
390 eukaryotes, the essential function of PfGRP170 may not be entirely linked to its role in
391 regulating BiP.
392
393 We utilized two separate IP/mass spectroscopy approaches to generate a list of 11 high-
394 confidence interacting partners of PfGRP170. Seven of the proteins (including PfBiP)
395 have a peak expression pattern around the time PfGRP170-GFP-DDD parasites begin to
396 die. SERA5 and SERA6 have been shown to be required for egress from the RBC, which
397 would be after the PfGRP170-GFP-DDD parasites die[69-71]. RON3 has been shown to
398 been suggested to be a protein important for RBC invasion, which implies this protein

399 interaction is also not why PfGRP170-GFP-DDD parasites are dying[72]. CLAG9, another
400 identified protein, has been proposed to play a role in cytoadherence to CD36 and
401 remodeling the host RBC after invasion by a merozoite[73,74]. PDI-11 was predicted to be
402 non-essential in a *piggyBac* mutagenesis conducted in *Plasmodium*[75]. The remaining
403 protein was parasite-infected erythrocyte surface protein 1 (PIESP1). Overexpression
404 data suggest that PIESP1 is exported to the host RBC[76]. However, this protein has a
405 putative ER retention signal (TDEL). These last four amino acids were left off of the GFP
406 fusion protein that was expressed in the parasite as the authors predicted this protein was
407 a transmembrane protein and thus leaving off these amino acids would have no effect on
408 protein localization[76]. Further studies will be needed to determine the precise subcellular
409 localization of PIESP1 and determine its role in parasite biology. These data show that
410 PfGRP170 is essential for the asexual lifecycle of *P. falciparum* and that the biological
411 role of PfGRP170 is quite divergent from other eukaryotes. Further, given the divergence
412 between mammalian and parasite GRP170s, PfGRP170 could be a viable antimalarial
413 drug target.
414
415

416 ***FIGURES***

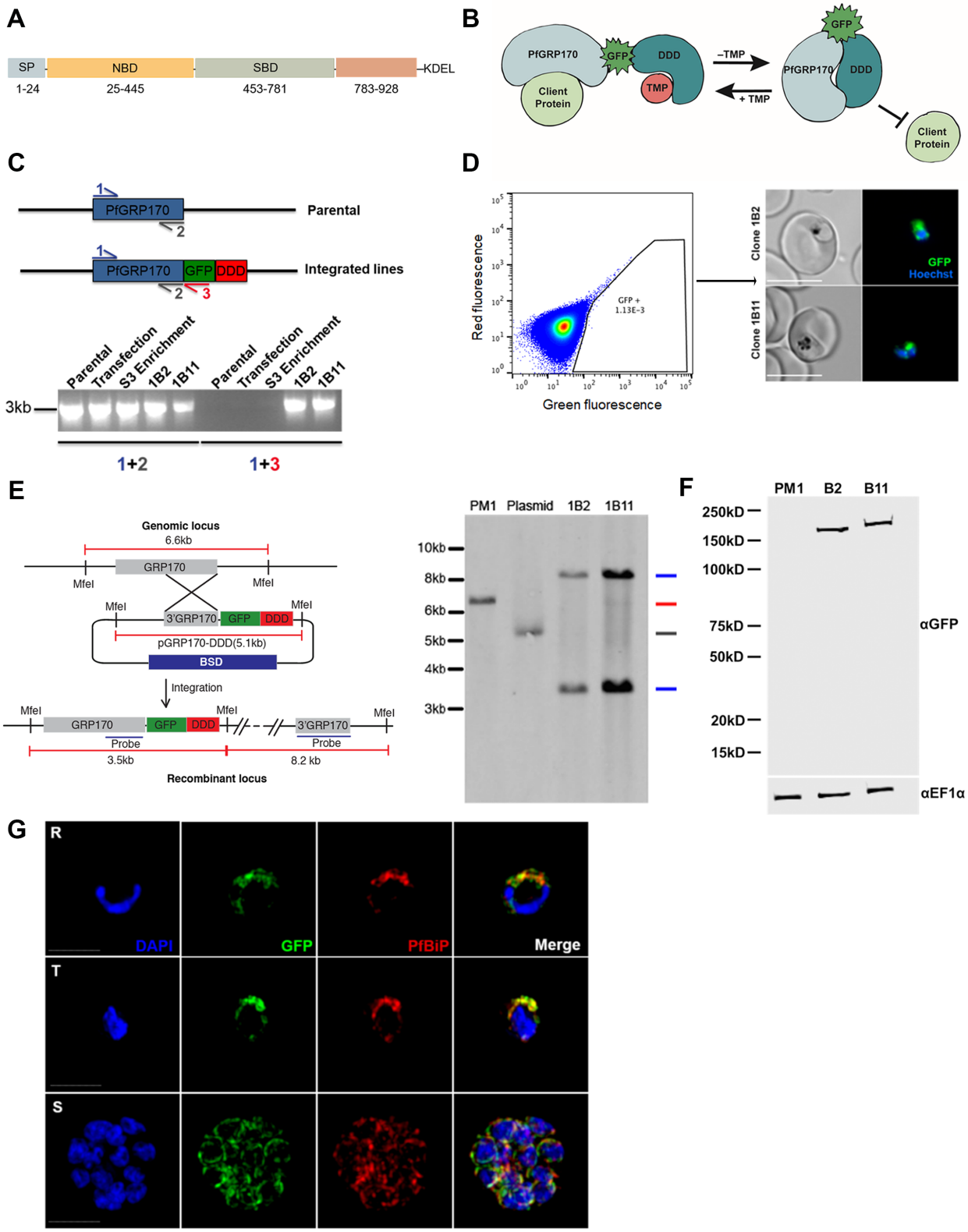

417

418 **Figure 1: Generation of PfGRP170-GFP-DD Parasites**

419 **(A).** Schematic detailing the putative domain boundaries of PfGRP170 (PF3D7_1344200)
420 based on the yeast homolog, Lhs1: Signal Peptide (SP), Nucleotide Binding Domain
421 (NBD), Substrate Binding Domain (SBD), Extended C-terminus region (783-928), and an
422 ER retention signal (KDEL).
423 **(B).** Schematic diagram demonstrating the conditional inhibition of PfGRP170.
424 Conditional inhibition of PfGRP170 is achieved by the removal of Trimethoprim (TMP),
425 which results in the unfolding of the destabilization (DDD). The chaperone recognizes
426 and binds the unfolded DDD and is inhibited from interacting with client proteins.
427 **(C)**. **(Top)** Schematic diagram of the PfGRP170 locus in the parental line (PM1KO) and
428 the modified locus where PfGRP170 is endogenously tagged with GFP and DDD. Primers
429 used for integration test and control PCR are indicated by arrows. The relative positions
430 of Primer 1 (blue) and Primer 2 (Gray) on the PfGRP170 locus are shown. These two
431 primers will amplify PfGRP170 in parental and transfected parasites. Primer 3 (Red)
432 recognizes the GFP sequence. Primers 1 and 3 were used to screen for proper integration
433 into the PfGRP170 locus. **(Bottom)** PCR integration test and control PCRs on gDNA
434 isolated from the PM1KO (parental), the original transfection of the pPfGRP170-GFP-
435 DDD plasmid after three rounds of Blasticidin (BSD) drug selection (Transfection), the
436 PfGRP170-GFP-DDD transfected parasite lines after two rounds of enrichment for GFP
437 positive cells (S3 enrichment), and PfGRP170-GFP-DDD clones 1B2 and 1B11 after
438 MoFlo XDP flow sorting. The first 5 lanes are control PCRs using primers to amplify the
439 PfGRP170 locus. The last 5 lanes are integration PCRs that only amplify if the GFP-DDD
440 has been integrated into the genome.
441 **(D). (Left)** MoFlo XDP flow data demonstrating the percentage of GFP positive parasites
442 in transfected PfGRP170-GFP-DDD parasites following three rounds of drug selection
443 with Blasticidin (BSD) and two rounds of enrichment with an S3 cell sorter. Using the
444 MoFlo, single GFP positive cells were cloned into a 96 well plate. Two clones, 1B2 and
445 1B11, were isolated using this method. **(Right)** 1B2 and 1B11 parasites, were observed
446 using live fluorescence microscopy.
447 **(E).** Southern blot analysis of PfGRP170-GFP-DDD clones 1B2 and 1B11, PM1KO
448 (parental control), and the PfGRP170-GDB plasmid is shown. Mfe1 restriction sites, the
449 probe used to detect the DNA fragments, and the expected sizes are denoted in the

450 schematic **(Left).** Expected sizes for PfGRP170-GFP-DDD clones (blue), parental DNA
451 (red), and plasmid (gray) were observed **(Right).** Parental and plasmid bands were
452 absent from the PfGRP170-GFP-DDD clonal cell lines.
453 **(F).** Western blot analysis of protein lysates from PM1KO (parental) and PfGRP170-GFP-
454 DDD clonal cell lines 1B2 and 1B11 is shown. Lysates were probed with anti-GFP to
455 visualize PfGRP170 and anti-PfEF1α as a loading control.
456 **(G).** Asynchronous PfGRP170-GFP-DDD parasites were paraformaldehyde fixed and
457 stained with anti-GFP, anti-PfGRP78 (BiP), and DAPI to visualize the nucleus. Images
458 were taken as a Z-stack using super resolution microscopy and SIM processing was
459 performed on the Z-stacks. Images are displayed as a maximum intensity projection. The
460 scale bar is 2μm.
461

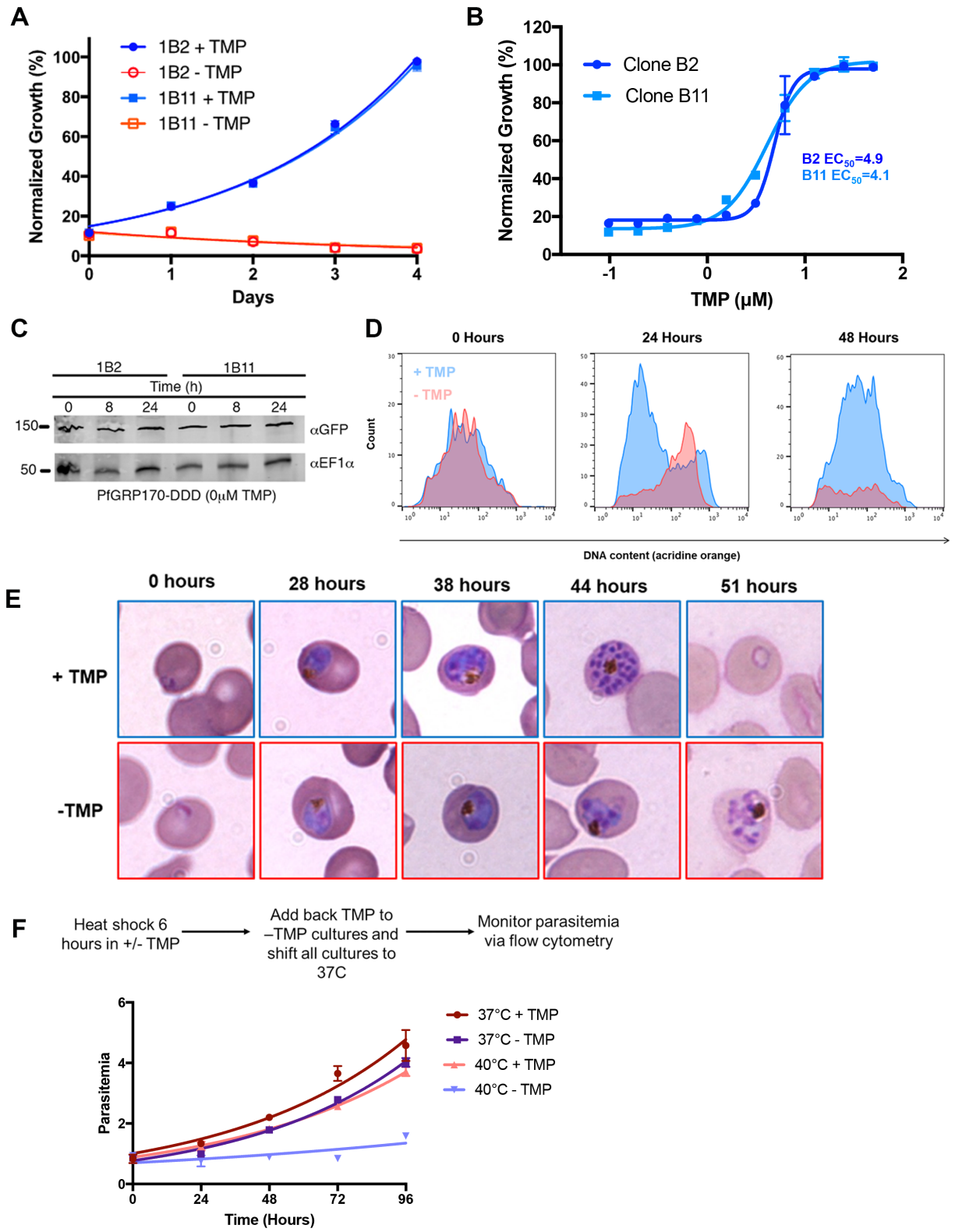

Figure 2: PfGRP170 is Essential and Required for Surviving a Heat Shock

464 **(A).** Growth of asynchronous PfGRP170-GFP-DDD clonal cell lines 1B2 and 1B11, in the
465 presence or absence of 20μM TMP, was observed using flow cytometry over 4 days. One
466 hundred percent growth is defined as the highest parasitemia in samples with TMP, on
467 the final day of the experiment. Data was fit to an exponential growth curve equation.
468 Each data point is representative of the mean of 3 replicates ± S.E.M.
469 **(B).** Asynchronous PfGRP170-GFP-DDD clonal cell lines 1B2 and 1B11 were grown in a
470 range of TMP concentrations for 48 hours. After 48 hours, parasitemia was observed
471 using flow cytometry. One hundred percent growth is defined as the highest parasitemia
472 in the presence of TMP on the final day of the experiment. Data was fit to a dose-
473 response equation. Each data point is representative of the mean of 3 replicates ± S.E.M.
474 **(C).** Western blot analysis of PfGRP170-GFP-DDD lysates at 0, 8, and 24 hours following
475 the removal of TMP is shown. Lysates were probed with anti-GFP to visualize PfGRP170
476 and anti-PfEF1α as a loading control.
477 **(D).** Flow cytometric analysis of asynchronous PfGRP170-GFP-DDD parasites,
478 incubated with (Blue) and without TMP (Red), and stained with acridine orange. Data at
479 0, 24, and 48 hours after the removal of TMP are shown.
480 **(E).** TMP was removed from tightly synchronized PfGRP170-GFP-DDD ring stage
481 parasites and their growth and development through the life cycle was monitored by
482 Hema 3 stained thin blood smears. Representative images are shown from the parasite
483 culture at the designated times.
484 **(F).** PfGRP170-GFP-DDD clones 1B2 and 1B11 were incubated with and without TMP
485 for 6 hours at either 37°C or 40°C. Following the incubation, TMP was added back to all
486 cultures and parasites were shifted back to 37°C. Parasitemia was then observed over
487 96 hours via flow cytometry. Data was fit to an exponential growth curve equation. Each
488 data point shows the mean of 3 replicates ± S.E.M.
489

A

Protein	PATS Score	PlasmoAP Score
PfGRP170	Very Likely (0.943/1)	Very likely (5/5 tests positive)

B

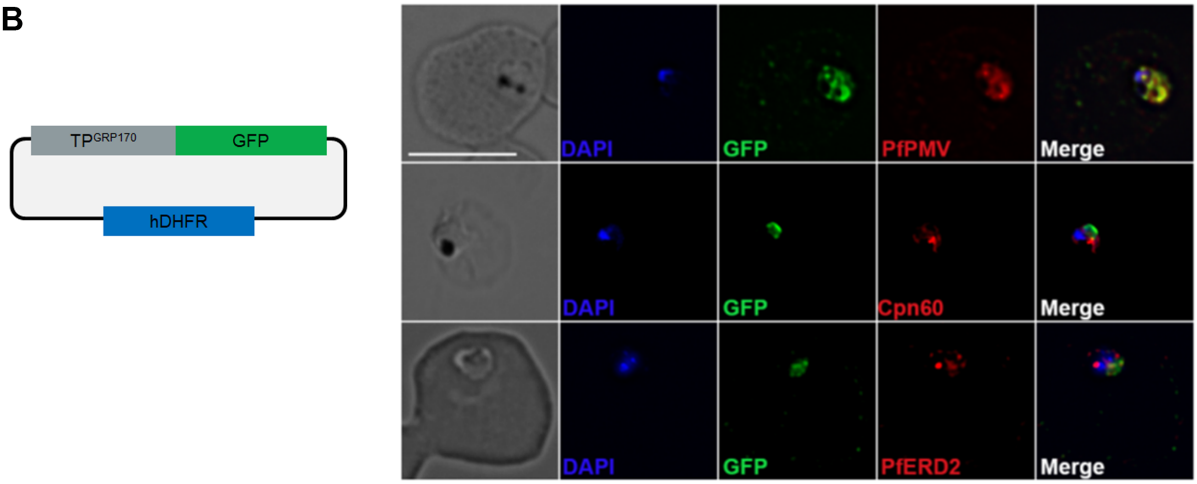

C

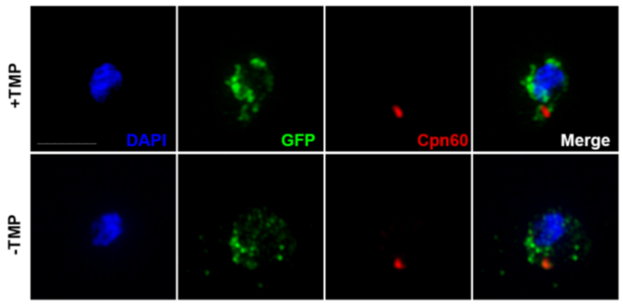

D

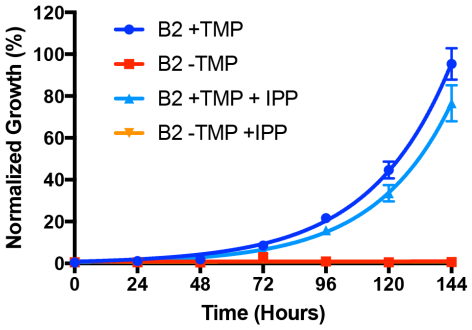

Figure 3: Putative PfGRP170 apicoplast transit peptide localizes to the ER and conditional inhibition of PfGRP170 does not affect trafficking of apicoplast proteins.

(A). Analysis of PfGRP170's protein sequence using two apicoplast transit peptide prediction programs: Prediction of Apicoplast-Targeted Sequences (PATS) and PlasmoAP.

(B). PfGRP170's putative apicoplast transit peptide was fused to GFP and transfected into 3D7 parasites. Parasites were fixed with acetone and stained with DAPI, anti-GFP

499 (to label the PfGRP170 putative transit peptide) and either anti-PfPMV (ER), anti-PfERD2
500 (Golgi), or anti-Cpn60 (Apicoplast) to determine subcellular localization. The images were
501 taken with Delta Vision II, deconvolved, and are displayed as a maximum intensity
502 projection. The scale bar is 5μm.
503 **(C).** Synchronized ring stage PfGRP170 parasites were incubated for 24 hours with and
504 without TMP. Following the incubation, the parasites were fixed with paraformaldehyde
505 and stained with DAPI, anti-GFP (PfGRP170) and anti-Cpn60 (Apicoplast). Images were
506 taken as a Z-stack using super resolution microscopy and SIM processing was performed
507 on the Z-stacks. Images are displayed as a maximum intensity projection. The scale bar
508 is 2μm.
509 **(D).** Asynchronous PfGRP170-GFP-DDD parasites were incubated with and without TMP
510 and in the presence or absence of 200μM IPP. Parasitemia was monitored using flow
511 cytometry for 144 hours. One hundred percent growth is defined as the highest
512 parasitemia in the presence of TMP, on the final day of the experiment. Data was fit to
513 an exponential growth curve equation. Each data point is representative of the mean of 3
514 replicates ± S.E.M.
515

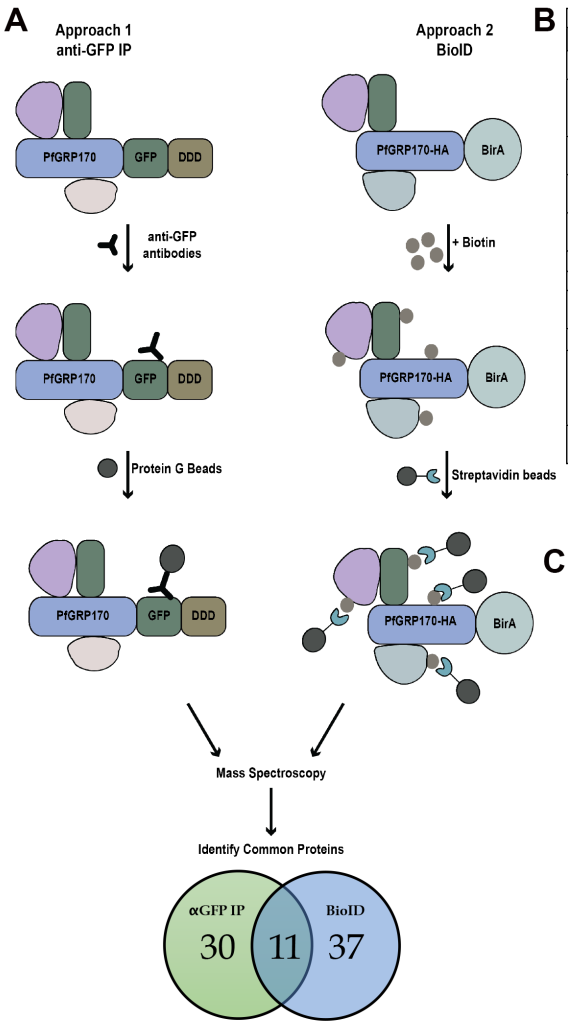

B

			Unique Peptides	
Gene ID	**Gene Product**	**Localization**	**IP (B2, B11)**	**BioID (1, 2)**
PF3D7_0917900	*Heat shock protein 70	ER	83, 80	27, 30
PF3D7_0310400	Parasite-infected erythrocyte surface protein	ER?	13, 12	17, 13
PF3D7_1134100	Protein disulfide isomerase	ER	4, 3	6, 3
PF3D7_1116800	Heat shock protein 101	Dense Granule	10, 14	4, 9
PF3D7_1129100	Parasitophorous vacuolar protein 1	Dense Granule	5, 6	5, 3
PF3D7_0207600	Serine repeat antigen 5	PV	14, 7	11, 5
PF3D7_0207500	Serine repeat antigen 6	PV	2, 3	2, 1
PF3D7_0935800	Cytoadherence linked asexual protein 9	Rhoptry	9, 8	8, 5
PF3D7_1252100	Rhoptry neck protein 3	Rhoptry	22, 16	23, 14
PF3D7_0505700	Conserved Plasmodium membrane protein, unknown function	Unknown	32, 31	41, 39
PF3D7_1462300	GTP-binding protein, putative	Unknown	9, 10	26, 21

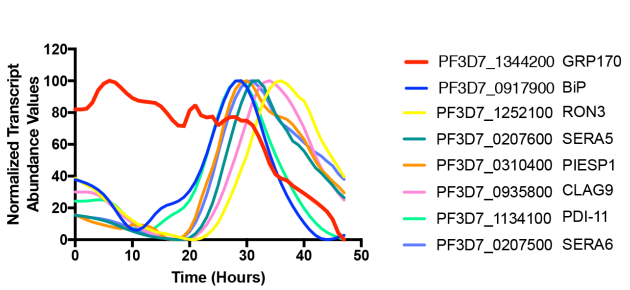

Figure 4: PfGRP170 interacting partners

(A). Schematic diagram illustrating the two independent methods used to identify potential interacting partners of PfGRP170: anti-GFP Immunoprecipitation (IP) using lysates from PfGRP170-GFP-DDD parasites and streptavidin IP of PfGRP170-BirA parasites incubated with biotin for 24 hours followed by mass spectroscopy. The proteins identified from each IP were filtered to include only proteins that had a signal peptide and/or transmembrane domain using PlasmoDB. Proteins found in the respective control IP's (excluding PfBiP) were also removed from further analysis (data in Supplemental Table 1).

(B). The 11 proteins identified in both independent mass spectroscopy approaches (See Figure 4A and Supplemental Table 1). The PlasmoDB gene ID, gene product, putative

528 subcellular localization, and number of unique peptides identified for each protein in each
529 independent experiment are listed.
530 **(C).** The relative transcript abundance of interacting proteins, with peak expression
531 around the time the PfGRP170-GFP-DDD parasites die (36-44 hours), are plotted using
532 genome-wide real-time transcript data[46].
533

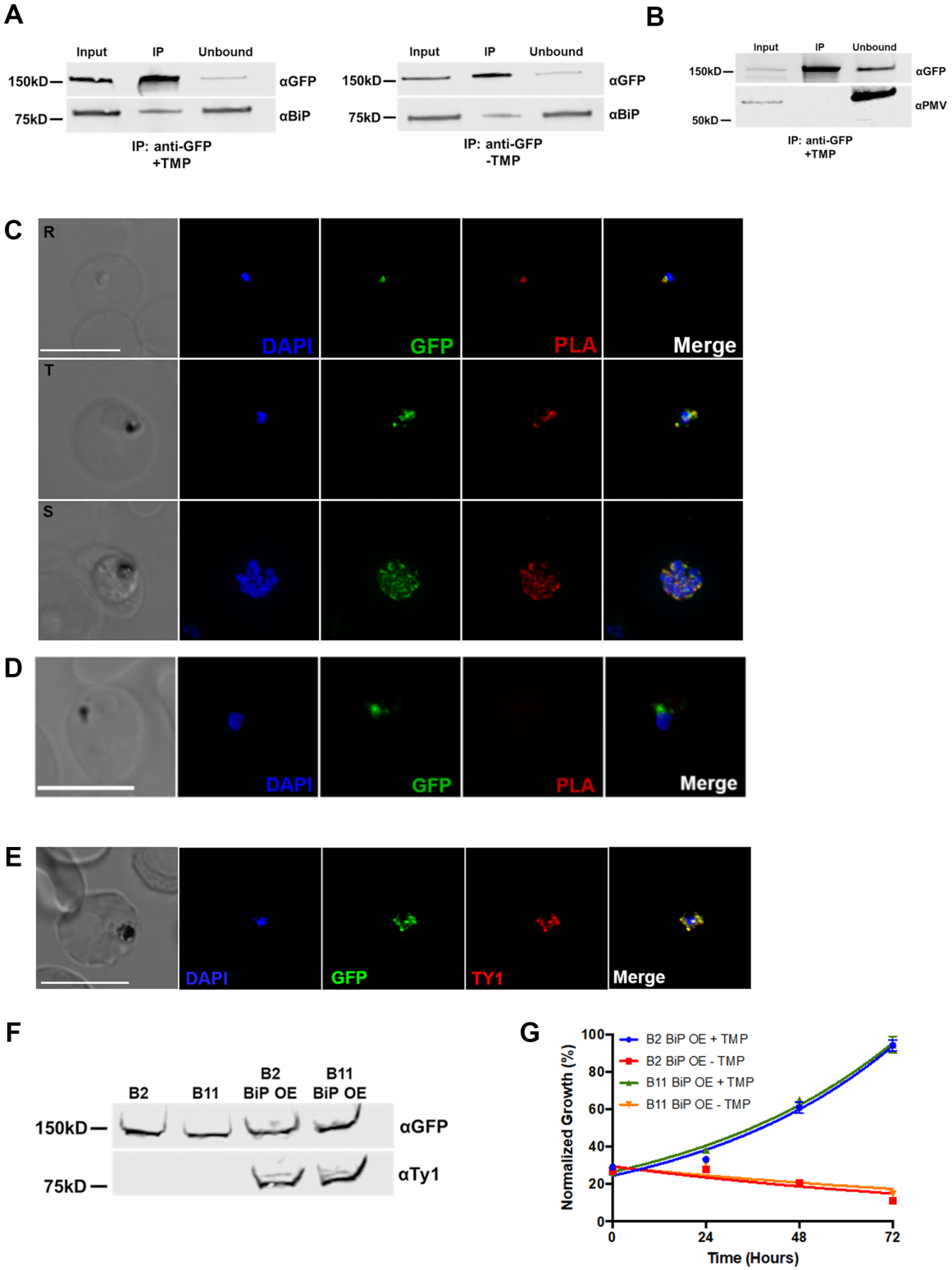

534

535 **Figure 5: PfGRP170 Interacts with BiP**

536 **(A)** Synchronized ring stage PfGRP170-GFP-DDD parasites were incubated with and
537 without TMP for 24 hours. Following this incubation, an anti-GFP IP was performed and
538 input, IP, and unbound fractions were analyzed using a western blot. The blot was
539 probed using anti-GFP and anti-BiP.
540 **(B).** Western blot analysis of an anti-GFP IP performed on asynchronous PfGRP170-
541 GFP-DDD parasites. Input, IP, and unbound fractions are shown. The blot was probed
542 using anti-GFP and anti-PfPMV.
543 **(C).** *In vivo* interaction of PfGRP170 and BiP. PfGRP170-GFP-DDD parasites were
544 paraformaldehyde fixed and stained with anti-GFP and anti-BiP. A Proximity Ligation
545 Assay (PLA) was then performed. The scale bar is 5μm. A negative control using anti-
546 GFP and anti-PfPMV is shown in **(D).**
547 **(E).** Asynchronous PfGRP170-GFP-DDD parasites overexpressing PfBiP-Ty1were
548 paraformaldehyde fixed and stained with anti-GFP (PfGRP170), anti-Ty1 (PfBiP-Ty1-
549 KDEL), and DAPI to visualize the nucleus. The images were taken with Delta Vision II,
550 deconvolved, and are displayed as a maximum intensity projection. The scale bar is 5μm.
551 **(F).** Western blot analysis of protein lysates from parental 1B2 and 1B11 parasites as well
552 as 1B2 and 1B11 parasites overexpressing the PfBiP-Ty1fusion protein. Lysates were
553 probed with anti-GFP to visualize PfGRP170 and anti-Ty1 to visualize PfBiP-Ty1-KDEL.
554 **(G).** Parasitemia of asynchronous PfGRP170-GFP-DDD parasites expressing PfBiP-Ty1-
555 KDEL, in the presence or absence of 20μM TMP, was observed using flow cytometry
556 over 3 days. One hundred percent growth is defined as the highest parasitemia on the
557 final day of the experiment. Data was fit to an exponential growth curve equation. Each
558 data point is representative of the mean of 3 replicates ± S.E.M.
559

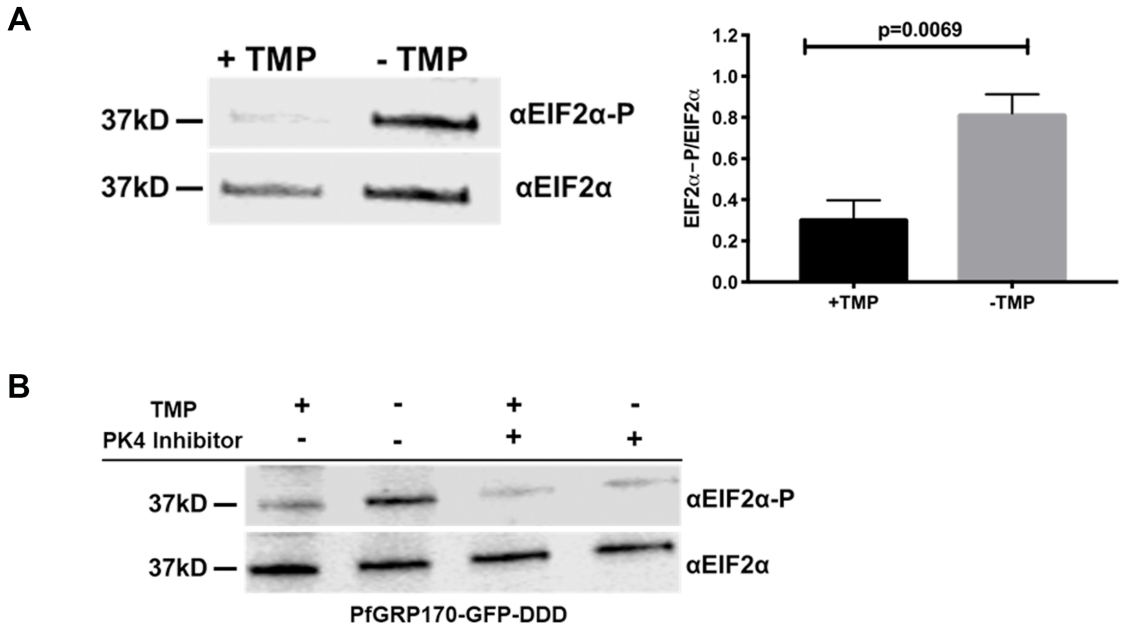

Figure 6: Loss of PfGRP170 function activates the PK4 stress pathway

(A). (Left) Synchronized ring stage PfGRP170-GFP-DDD parasites were incubated with and without TMP for 24 hours. Protein was isolated from these samples and analyzed via western blot, probing for anti-eIF2α and anti-Phospho-eIF2α. **(Right)** The ratio of phosphorylated EIF2α over total EIF2α for PfGRP170-GFP-DDD parasites incubated with and without TMP is shown. Western blot band intensities were calculated using ImageJ software (NIH) and the significance was calculated using an unpaired t test. Data are representative of 4 biological replicates ± S.E.M.

(B). Synchronized ring stage PfGRP170-GFP-DDD parasites were incubated with and without TMP and in the presence and absence of 2μM PK4 inhibitor GSK2606414 for 24 hours. Protein was isolated from these samples and analyzed via western blot by probing for anti-eIF2a and anti-Phospho-eIF2α.

```
Lhs1              1 MRNVLRLLFLTAFVAIGSL----AAVLGVDYGGQNIKAIVVSPQAPLELV     46
                    ||....|..|.......||    :::||:|:|.:.||..:|||.....::
PfGRP170          1 MRPRFFLFLLFIIYIYNSLRIKCSSLLGIDFGNEYIKVSIVSPGKGFNIL     50

Lhs1             47 LTPEAKRKEISGLSI-KRLPGYGKDDPNGIERIYGSAVGSLATRFPQNTL     95
                    |..::|||..:.:|. .:...|.::     .:||       :|::||.||
PfGRP170         51 LNNQSKRKITNSISFANKFRTYDEE-----SKIY-------STKYPQLTL     88

Lhs1             96 LHLKPLLGKSLEDETTVTLYSKQHPGLEMVSTNRSTIAFLVDNVEYPLEE    145
                    |:...:||.:|.|    :|.:|::              |:::|.:...||
PfGRP170         89 LNSNNILGYNLFD----SLKNKEN--------------FVIENYDENNEE    120

Lhs1            146 LVA-MNVQEIAN------------------RANSLLKDR--------DAR    168
                    ..: :|..:.:|                  ..|..|||.        .|.
PfGRP170        121 FYSDINNYDFSNDFGSKYYSYDYVVDHKRGTINIKLKDNMVISSEEVTAN    170

Lhs1            169 TEDFVNKMSFT---------------------IPDFFDQHQRKALLDASS    197
                    ...::.|:::|                     :|..|.|.:::||::||.
PfGRP170        171 ILGYIKKLAYTHLNIDYKVKRNINLNIGCVISVPCNFSQRKKQALINASK    220

Lhs1            198 ITTGIEETYLVSEGMSVAVNFVLKQRQFPPGEQQHYIVYDMGSGSIKASM    247
                    | .|:|...:::...:.|::.|   ...|....:..:..|:||.:|...:
PfGRP170        221 I-AGLELLGIINGVTAAAIHNV---HDIPLNTTKLTMYLDIGSKNINVGI    266

Lhs1            248 FSI-LQPEDTTQPVTIEFEGYGYNPHLGGAKFTMDIGSLIENKFLETH-P    295
                    .:| ...:|..:..:::.........:..|.|..|.:...:..||.|.: .
PfGRP170        267 ATISFVEKDKVRSRSVQVYACESLENNSGNKIDMLLAENLRKKFEEKYNV    316

Lhs1            296 AIRTDELHANPKALAKINQAAEKAKLILSANSEASINIESLINDIDFRTS    345
                    :|..|:     ||:.|:..||.||||:|||...|.:.||||.|:.....|
PfGRP170        317 SIENDK-----KAMRKLIVAANKAKLLLSAKKSADVFIESLYNNKSLNES    361

Lhs1            346 ITRQEFEEFIADSLLDIVKPINDAVTKQFGGYGTNLPEINGVILAGGSSR    395
                    ::||:|||.|.:.:.::..|||.|:.|  ||:  .|.:|..:.|.|...|
PfGRP170        362 VSRQDFEELIQEVIENMKIPINKALEK--GGF--QLKDIEALELIGSGWR    407

Lhs1            396 IPIVQDQLIKLVSEEKVLRNVNADESAVNGVVMRGIKLSNSFKTKPLNVV    445
                    :|.:.:::.:..:..||..::|:||:...|.:.....|.:|:.|.|:..
PfGRP170        408 VPKILNEVTEFFNPLKVGMHLNSDEAVTMGSLYIAAYNSANFRLKDLDYK    457

Lhs1            446 DRSVNTYSFKLSNESE------------LYDVFTRGSAYP-NKTSILTNT    482
                    |...|.|...::.:.|            ..::....|.|| ||..|||
PfGRP170        458 DIVSNEYHILVNTDEEENNTTNEEKVNIKKELVNYNSRYPHNKNVILT--    505

Lhs1            483 TDSIPNNFTIDLFENGKLFETITVNS--GAIKNSY---SSDKCSSGVAYN    527
                       ..:|....::||||:.....:.:  .|||:.|   .:.|      .|
PfGRP170        506 ---YKDNLKFSVYENGKIINEYVLGNLDNAIKSKYEHLGTPK------LN    546

Lhs1            528 ITFDLSSDRLFSIQEVNCICQSEND-IGNSKQIK----------------    560
                    :.|.|....:.|:.:|..:.:.:.| .|::|..|
PfGRP170        547 LKFHLDKFGILSLDKVLVVYEEQKDGAGDTKDNKKEGDEENNNNNNNEEI    596

Lhs1            561 ---------------NKGSR------------------------------    565
                                    |||..
PfGRP170        597 NKDDDTNNNKSDDEQNKGDENKSNDENKENEENKQNGEKKNDIIKHNIP    646

Lhs1            566 LAFTSEDVEIKRLSPSERSRLHEHIKLLDKQDKERFQFQENLNVLESNLY    615
                    :.|.:.:::...|:..|.....|.:|.||:.|.:.|...|..|.|||.:|
PfGRP170        647 IEFQTRNIKPLPLTFEEIKEKKEILKNLDEHDIDIFLKSEKKNTLESFIY    696

Lhs1            616 DARNLLMDDEVMQNGPKSQVEELSEMVKVYLDWLEDASFDTDPEDIVSRI    665
                    :.|:.:..|...|...:....|....::.|.|||.... |...|::.::|
PfGRP170        697 ETRSKMKQDIYKQVTKEETRNEYLNKLEEYEDWLYTEK-DEPLENVSNKI    745

Lhs1            666 REIGILKKKIELYMDSAKEPLNSQQFKG-MLEEGHKLLQ-AIETHKNTVE    713
                    .|:.      ::| :..||.....|.:. ::||.:|.:| .||..|:
PfGRP170        746 HELQ------DIY-NPIKERAEELQVRDKIIEETNKKIQEMIEKIKD---    785

Lhs1            714 EFLSQFETEFADTIDNVREEFKKIKQPAYVSKALSTWEETLTSFKNSISE    763
                      ||:.:...|:||..|::.         :.|.:..|.......|    :
PfGRP170        786 --LSEKKPWAAETIKMVKDS---------LDKEVQWWNHAQEEQK----K    820

Lhs1            764 IEKFLAKNLFGEDLREHLFEIKLQFDMYRTKLEEKLRLIKSGDESRLNEI    813
                    ::.:.|.....:|      ::|:|...:       .|||:.|:.:....
PfGRP170        821 LDNYTAPFFKHKD-------VQLKFKSIQ-------MLIKTLDKLKKPVE    856

Lhs1            814 KKLHLRNFRLQKRKEEK-----------LKRKLEQEKSRNNNETESTVIN    852
                    ||...:|...|.....|           .:.:.||.....|||......|
PfGRP170        857 KKEDKKNTDNQNENTSKQDAGADKNHNTTENQNEQSAQNQNNENNDDNQN    906

Lhs1            853 SADDKTTIVNDKTTESNPSSEEDILHDEL    881
                    :..|.....||:..:::.:|::   .|||
PfGRP170        907 NEHDANQSSNDEQNKNDGASDQ---KDEL    932
```

Supplemental Figure 1: Sequence Alignment of Lhs1 and PfGRP170

576 Sequence alignment of *S. cerevisiae* GRP170 (Lhs1) and PfGRP170. The alignment was
577 performed using EMBOSS Needle which creates a global alignment of two sequences
578 using the Needleman-Wunsch algorithm. The software used to do this is provided by the
579 European Bioinformatics Institute, which is a part of the European Molecular Biology
580 Laboratory (EMBL). Identical residues are indicated by a "I", strongly similar residues are
581 indicated by a ":", and weakly similar residues are indicated by a ".".
582

Organism	% Identity	% Homology
P. vivax	62.6	78.6
P. malariae	65.5	81.7
P. ovale	61.7	77.5
P. berghei	59.6	77.5
T. gondii	26.2	45.5
S. cerevisiae	22.4	40.1
H. sapiens	23.6	42.1

583
584 **Supplemental Figure 2: Sequence homology of PfGRP170**
585 Sequence identify and homology of *P. falciparum* GRP170 compared to GRP170
586 homologs from other *Plasmodium* Species (*P. vivax (*PVX_083105), *P. malariae*
587 *(*PmUG01_12020700), *P. ovale (*PocGH01_12018900), and *P. berghei*
588 *(*PBANKA_1357200)), *T. gondii* GRP170 (TGGT1_226830), yeast GRP170 (*S.*
589 *cerevisiae*), and human GRP170 (*H. sapiens*). Alignments to determine sequence identify
590 and homology were performed using EMBOSS Needle which creates a global alignment
591 of two sequences using the Needleman-Wunsch algorithm. The software to do this is
592 provided by the European Bioinformatics Institute, which is a part of the European
593 Molecular Biology Laboratory (EMBL).
594

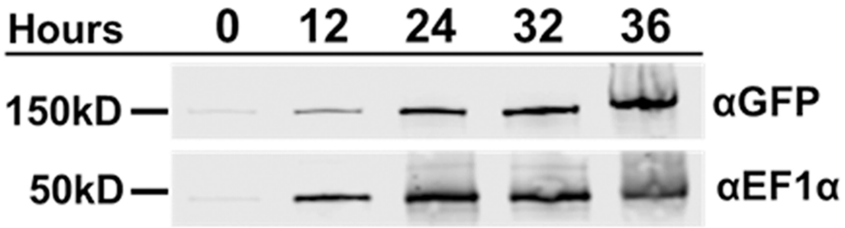

Supplemental Figure 3: PfGRP170 is Expressed Throughout the Asexual Life Cycle TMP was removed from tightly synchronized ring stage PfGRP170-GFP-DDD parasites and protein was isolated throughout the asexual life cycle. Lysates were separated on a Western blot and probed with anti-GFP to visualize PfGRP170-GFP-DDD and anti-PfEF1α as a loading control.

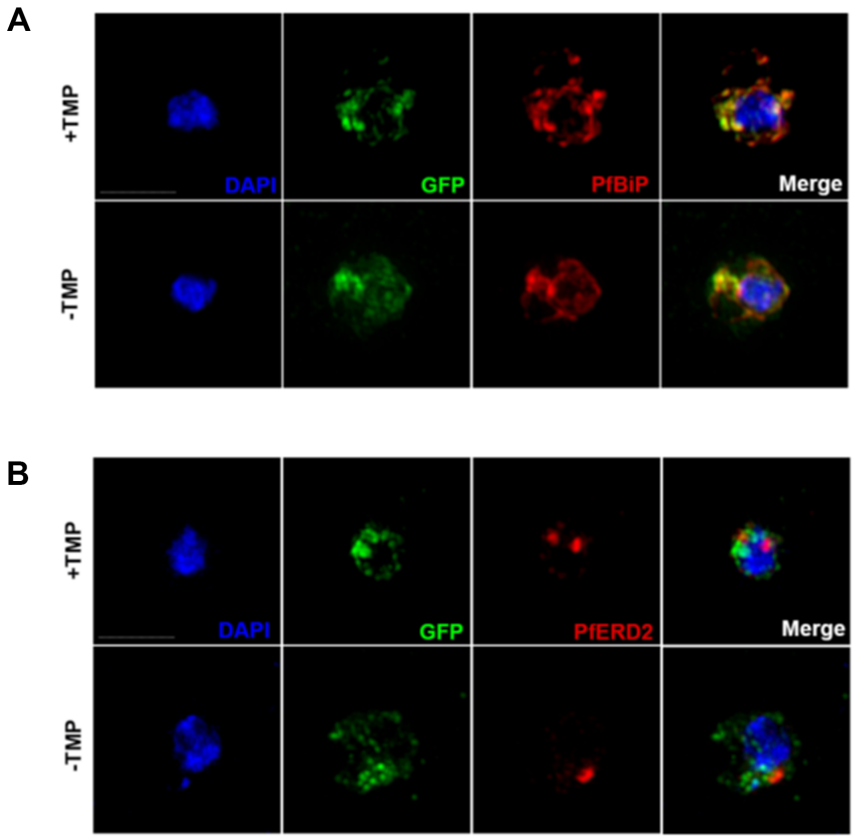

602

603 **Supplemental Figure 4: Conditional mutants of PfGRP170 localize to the ER**

604 Synchronized PfGRP170-GFP-DDD ring stage parasites were incubated with and without
605 TMP for 24 hours. Parasites were then fixed with paraformaldehyde and stained with
606 either DAPI, anti-GFP, and anti-BiP (ER) **(A)** or DAPI, anti-GFP, and anti-ERD2 (Golgi)
607 **(B).** Images were taken as a Z-stack using super resolution microscopy and SIM
608 processing was performed on the Z-stacks. Images are displayed as a maximum intensity
609 projection. The scale bar is 2μm.

610

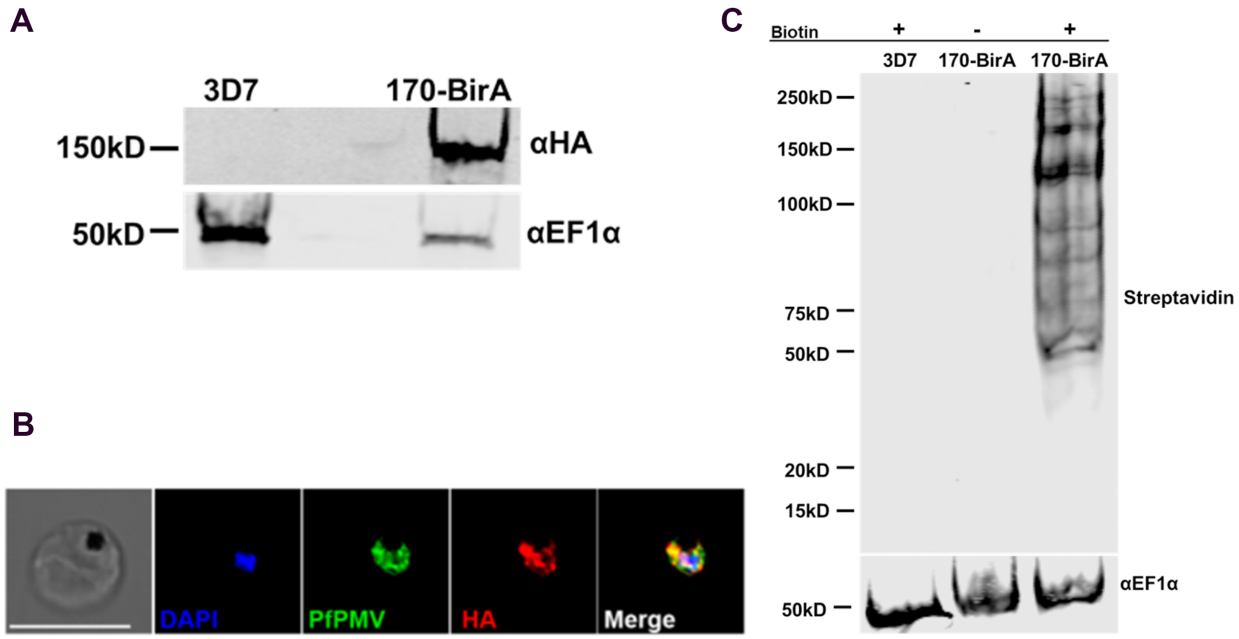

611

612 **Supplemental Figure 5: PfGRP170-BirA localizes to the parasite ER and**
613 **biotinylates proteins.**
614 **(A).** Western blot of 3D7 (parental) and PfGRP170-BirA expressing parasites probed with
615 anti-HA and anti-EF1α.
616 **(B).** Paraformaldehyde fixed PfGRP170-BirA parasites stained with anti-HA (PfGRP170-
617 BirA), anti-PfPMV (ER), and DAPI. The images were taken with Delta Vision II,
618 deconvolved and are displayed as a maximum intensity projection. The scale bar is 5μm.
619 **(C).** A western blot analysis of 3D7 (parental) and PfGRP170-BirA parasites following a
620 24-hour incubation with biotin is shown. A fluorophore-labeled streptavidin secondary
621 antibody was used to visualize biotinylated proteins. A control with PfGRP170-BirA
622 parasites incubated without biotin is also shown. Anti-EF1α is used as a loading control.
623

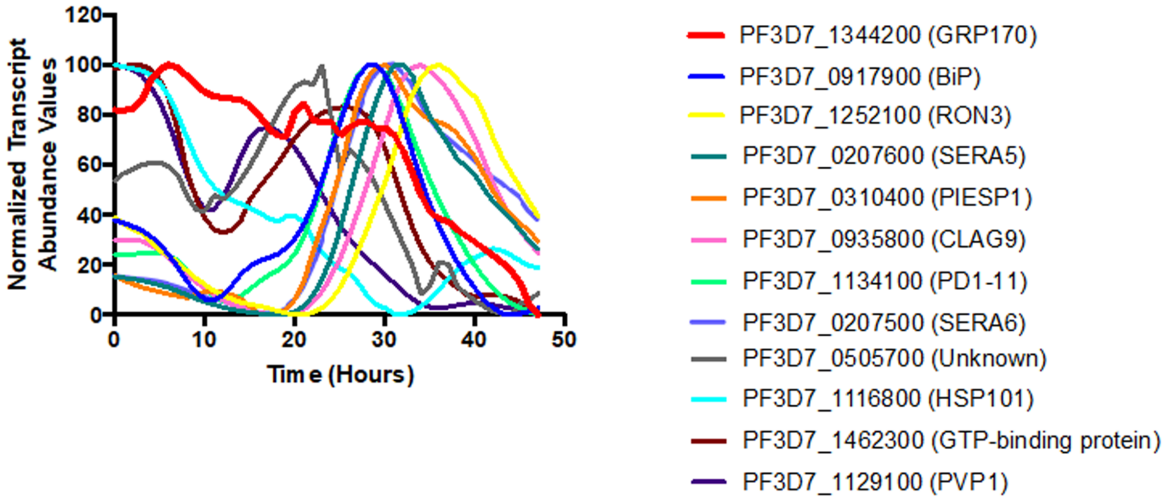

Supplemental Figure 6: Relative transcript abundance of proteins identified in both the anti-GFP co-immunoprecipitation and BioID mass spectroscopy approaches

The relative transcript abundance of the 11 PfGRP170 interacting proteins identified in Figure 4. The data are plotted using previously published genome-wide real-time transcription data[46].

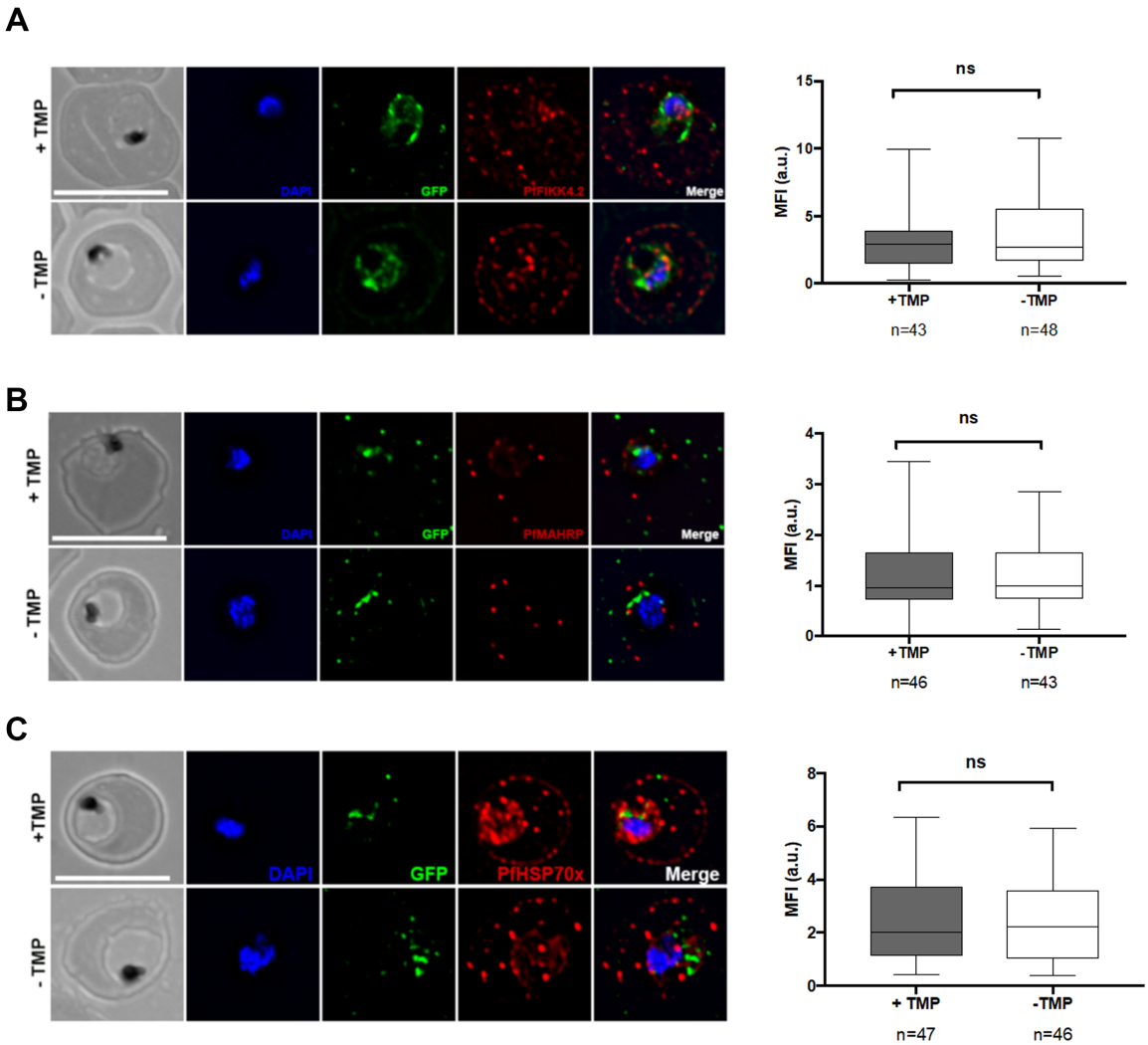

Supplemental Figure 7: PfGRP170 is not Required for Trafficking to the Host RBC. Tightly synchronized ring stage PfGRP170-GFP-DDD parasites were incubated with and without TMP for 24 hours. Following this incubation, parasites were fixed with acetone and stained with DAPI, anti-GFP (PfGRP170) and either anti-PfFIKK4.2 **(A),** anti-PfMAHRP1C **(B),** or anti-PfHSP70X **(C).** The images were taken with Delta Vision II, deconvolved, and are displayed as a maximum intensity projection. The scale bar is 5μM. Mean Fluorescent Intensity (M.F.I) was calculated for the exported fraction (PfFIKK4.2, PfMAHRP1C, and PfHSP70x) from individual cells. Data are from two independent

639 experiments and is displayed as box-and-whiskers plots (whiskers represent the
640 maximum and minimum M.F.I). The significance was calculated using an unpaired t test
641 (NS= not significant).
642

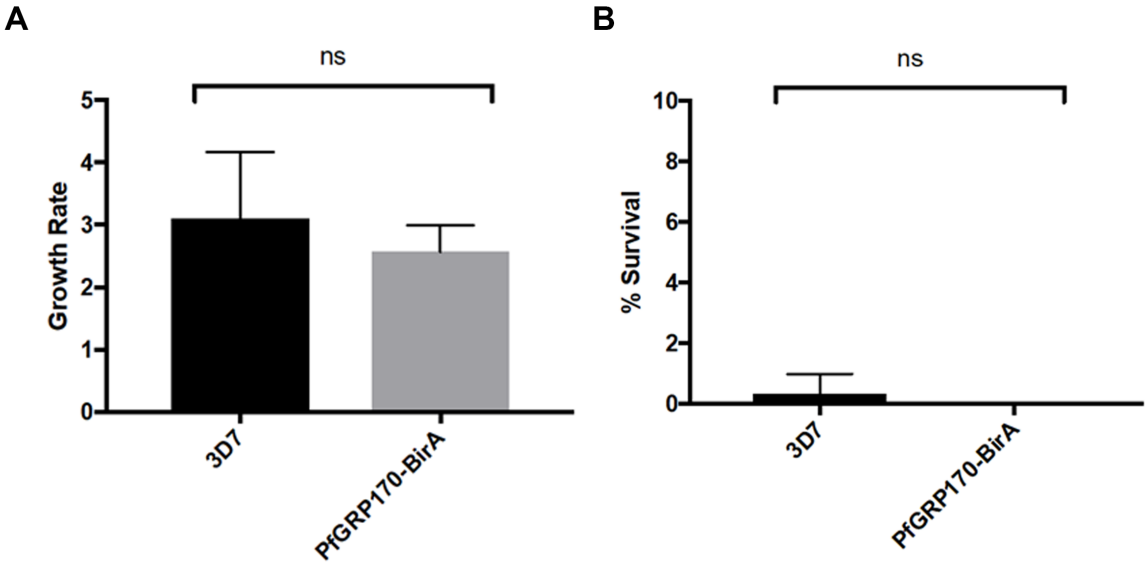

643
644 **Supplemental Figure 8: Overexpression of PfGRP170 does not Confer Artemisinin**
645 **Resistance**
646 Tightly synchronized ring stage 3D7 and PfGRP170-BirA parasites were incubated with
647 either 1% DMSO (Control) or Dihydroartemsinin (DHA) for 6 hours. After 6 hours the drug
648 is removed by washing the culture with complete RPMI. Parasitemia was calculated using
649 Giemsa stained thin blood smears at 0 hours (to calculate starting parasitemia) and 72
650 hours after either DMSO or DHA exposure. Four independent replicates of the experiment
651 were completed for 3D7 and three for PfGRP170-BirA. The growth rate of the 3D7 and
652 PfGRP170-BirA parasites, incubated only with DMSO, was calculated after 72 hours **(A).**
653 The percent survival of parasites was calculated for 3D7 and PfGRP170-BirA after DHA
654 exposure was calculated after 72 hours **(B).**
655

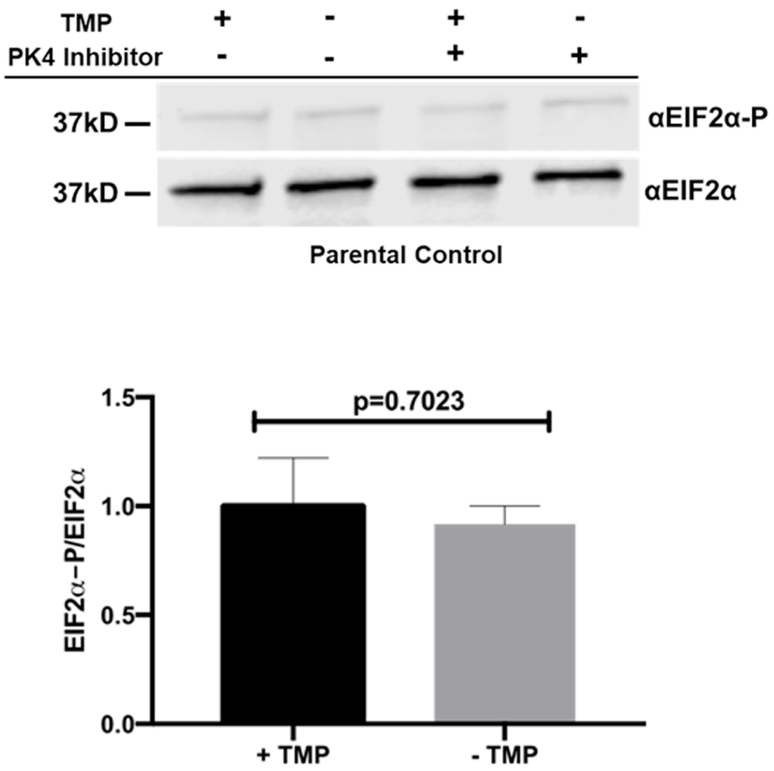

656

657 **Supplemental Figure 9: EIF2-α levels do not change in PM1 parasites in the**
658 **presence or absence of TMP or a PK4 inhibitor.**
659 **(Top)** Synchronized ring stage PM1 parasites were incubated with and without TMP and
660 in the presence and absence of 2μM PK4 inhibitor GSK2606414 for 24 hours. Protein
661 was isolated from these samples and analyzed via western blot by probing for anti-eIF2a
662 and anti-Phospho-eIF2α. **(Bottom)** The ratio of phosphorylated EIF2α over total EIF2α in
663 PM1 parasites incubated with and without TMP is shown. Western blot band intensities
664 were calculated using ImageJ software (NIH) and the significance was calculated using
665 an unpaired t test. Data are representative of 2 biological replicates ± S.E.M.

666

667 **Supplemental Table 1: Raw Mass Spectroscopy data**
668 Raw mass spectroscopy data from two anti-GFP IP (using 1B2 and 1B11), two parental
669 anti-GFP IP's (using PM1), two Streptavidin IP's the PfGRP170-BirA cell lines following a
670 24 incubation with biotin, and one streptavidin IP's of 3D7 cell lines following a 24 hour
671 incubation with biotin. Both approaches used asynchronous cells. The excel file includes

672 the following: A total list of proteins from PlasmoDB containing a signal peptide and/or
673 transmembrane domain used to sort the mass spectroscopy data (Tab 1), raw mass
674 spectroscopy data from PM1 anti-GFP IP's 1 and 2 (Tabs 2 and 3), list of proteins from
675 the PM1 anti-GFP IP's 1 and 2 that contained a signal peptide and/or transmembrane
676 domain (Tabs 4 and 5), raw mass spectroscopy data from the 1B2 anti-GFP IP (Tab 6)
677 and the list of proteins from the 1B2 anti-GFP IP that contained a signal peptide and/or
678 transmembrane domain (Tab 7), raw mass spectroscopy data from the 1B11 anti-GFP IP
679 (Tab 8) and the list of proteins from the 1B11 anti-GFP IP that contained a signal peptide
680 and/or transmembrane domain (Tab 9), raw mass spectroscopy data from a streptavidin
681 IP on 3D7 parasites incubated with biotin (Tab 10), the list of proteins from the 3D7
682 streptavidin IP that contained a signal peptide and/or transmembrane domain (Tab 11),
683 raw mass spectroscopy data from two independent PfGRP170-BirA streptavidin IP's
684 (Tabs 12 and 13) and the list of proteins from the PfGRP170-BirA streptavidin IP's that
685 contained a signal peptide and/or transmembrane domain (Tabs 14 and 15).
686

687 **ACKNOWLEDGMENTS**

688 We thank Dan Goldberg for anti-EF1α and anti-PMV antibodies; Boris Striepen for anti-
689 Cpn60 antibody; Hans-Peter Beck for anti-MAHRP antibody; Jude Przyborski for anti-
690 PfHSP70x antibody; David Cavanagh and EMRR for anti-FIKK4.2 antibody; Drew
691 Etheridge, Min Zhang, and Bill Sullivan for technical suggestions; Muthugapatti
692 Kandasamy at the University of Georgia Biomedical Microscopy Core, Julie Nelson at the
693 CTEGD Cytometry Shared Resource Lab for technical assistance. We acknowledge
694 assistance of the Emory University Integrated Proteomics Core for mass spectrometry.
695 This work was supported by ARCS Foundation awards to H.M.K. and D.W.C., UGA
696 Startup funds to V.M., CDC-UGA Seed Award to V.M. and N.W.L., and the US National
697 Institutes of Health (R00AI099156 and R01AI130139) to V.M. and (T32AI060546) to
698 H.M.K. and to M.A.F.
699

700 **METHODS**

701 ***Primers and Plasmid construction***

702 All primer sequences used in this study can be found in Supplemental Table 2.

703 Generation of pGDB-SDEL plasmid was done using the QuikChange II Site-Directed
704 Mutagenesis Kit (Agilent Technologies) on the pGDB plasmid with primers P1 and P2 per
705 the manufacturer's protocol[36].
706 Genomic DNA was isolated using the QIAamp DNA blood kit (Qiagen). gDNA used in this
707 study was isolated from either 3D7 or Plasmepsin I knockout parasites (PM1KO)[36]. The
708 pPfGRP170-GFP-DDD plasmid used to generate the PfGRP170-GFP-DDD mutants was
709 made by amplifying via PCR an approximately 1-kb region homologous to the 3'end of
710 the PfGRP170 gene (stop codon not included) using primers P3 and P4. The amplified
711 product was inserted into pGDB-SDEL plasmid using restriction sites Xho1 and AvrII
712 (New England Biolabs) and transformed into bacteria. The construct was sequenced prior
713 to transfection.
714
715 The pGRP170-HA-BirA-KDEL plasmid was prepared by amplifying PfGRP170 (without
716 the stop codon) from 3D7 gDNA using primers P5 and P6 and 3xHA-BirA from the
717 pTYEOE-3XHA-BirA plasmid (From D. Goldberg) using primers P7 and P8. Both PCR
718 products generated included homologous regions used for Sequence and Ligation
719 Independent Cloning (SLIC)[77] .The primers to amplify the 3xHA-BirA included the
720 sequence of an ER retention signal (KDEL). These PCR products were fused together
721 using PCR sewing as described previously and subsequently PCR amplified using
722 primers P5 and P8[35]. The resulting product was then inserted into pCEN-DHFR[78] that
723 was digested with Nhe1 and BglII (New England Biolabs) using SLIC and transformed
724 into bacteria as described previously[32,35].
725
726 The pPfGRP170TP-GFP plasmid was prepared by amplifying the first 450 bp (includes
727 the signal peptide and putative transit peptide sequence) of PfGRP170 from PM1 gDNA
728 using primers P5 and P9. The GFP sequence used was amplified from pGDB using
729 primers P10 and P11. The PfGRP170 transit peptide PCR was digested with Nhe1 and
730 AatII (New England Biolabs) and the GFP PCR was digested with AatII and BglII (New
731 England Biolabs). The two fragments were then ligated together (via the AatII digest site)
732 using a T4 ligase (kit from New England Biolabs) and subsequently PCR amplified using
733 primers P5 and P11. The resulting product was then digested with Nhe1 and BglII and

734 inserted into pCEN-DHFR[78] that was digested with Nhe1 and BglII (New England Biolabs)
735 using a T4 ligase and transformed into bacteria as described previously[32,35].
736
737 The pPfBiP-Ty1overexpression plasmid was prepared first by generating cDNA using the
738 SuperScript III reverse transcriptase kit (Invitrogen) using primer P14. PfBiP was then
739 amplified from the cDNA using primers P14 and P15. The resultant PCR product included
740 PfBiP, a single Ty1 tag, and an ER retention signal (KDEL). The pCEN vector was
741 modified to contain the DHOD resistance gene instead of the DHFR for parasite
742 selection[78]. The PfBiP-Ty1-KDEL-KDEL PCR was cloned into the pCEN-DHOD vector
743 cut with Nhe1 and BglII (New England Biolabs) using the IN-Fusion HD EcoDry Cloning
744 Kit (Clontech).
745
746 ***Cell Culture, transfections, and isolation of clonal cell lines***
747 Parasites were grown in RPMI 1640 media supplemented with Albumax 1 (Gibco) and
748 transfected as described previously[31-33,35,36].
749
750 To generate PfGRP170-GFP-DDD mutants, PM1KO parasites were transfected with the
751 pPfGRP170-GFP-DDD plasmid in duplicate. PM1KO parasites contain the human
752 dihydrofolate reductase (hDHFR) expression cassette which gives the parasites
753 resistance to Trimethoprim (TMP)[36]. Drug selection and cycling were performed as
754 described previously using 10μM TMP (Sigma) and 2.5μg/ml Blasticidin (Sigma)[32,33,36].
755 Following drug cycling, GFP positive cells were enriched using an S3 Cell Sorter
756 (BioRad). Individual GFP positive cells from a single transfection were cloned into 96 well
757 plates using a MoFlo XDP flow cytometer. After the EC_{50} of TMP was determined for
758 clones 1B2 and 1B11, parasites were shifted into media containing 2.5μg/ml BSD and
759 20μM TMP to facilitate optimal growth.
760
761 The PfGRP170-BirA and PfGRP170TP-GFP parasites were generated by transfecting
762 3D7 parasites with plasmids pGRP170-HA-BirA-KDEL or pPfGRP170TP-GFP,
763 respectively. Parasites expressing these episomal constructs were selected using 2.5nM
764 WR99210.

765

766 To generate the PfGRP170-GFP-DDD parasites episomally expressing PfBiP-Ty1-
767 KDEL-KDEL, PfGRP170-GFP-DDD clones 1B2 and 1B11 were each transfected with
768 pPfBiP-Ty1-KDEL. This plasmid expresses PfBiP-Ty1-KDEL using the *pbef1α* bi-
769 directional promoter. Parasites expressing this episomal construct were selected using
770 250nM of DSM1[79].

771

772 ***Integration tests for PfGRP170-GFP-DDD mutants***

773 Genomic DNA was isolated from parasites using the QIAamp DNA blood kit (Qiagen).
774 Control primers to amplify the genome were P4 and P12 and primers used to amplify
775 integrated DNA were P12 and P13.

776 Southern blot analysis was performed on DNA isolated from PfGRP170-GFP-DDD
777 parasites (1B2 and 1B11) as described previously[32,35]. The assay was also performed on
778 PM1KO parental DNA and the pGRP170-DDD plasmid as a control. DNA was isolated
779 from parasites using the QIAamp DNA blood kit (Qiagen). 10µg of precipitated PM1KO
780 DNA, 1B2, and 1B11 DNA and 10ng of pGRP170-DDD plasmid was digested overnight
781 with Mfe1 (New England Biolabs). The biotinylated probe used was generated by PCR
782 using biotinylated-16-UTP (Sigma) and primers P3 and P4. The biotinylated probe on the
783 southern blot was detected using IRDye 800CW streptavidin-conjugated dye (LICOR
784 Biosciences) and imaged using the Odyssey infrared imaging system (LICOR
785 Biosciences).

786

787 ***Growth assays using flow cytometry***

788 TMP was removed from asynchronous PfGRP170-GFP-DDD cultures for growth assays
789 by washing the culture in equal volume of complete RPMI three times. The culture was
790 then resuspended in complete RMPI media containing either 2.5µg/ml Blasticidin (Sigma)
791 for conditional inhibition (Sigma) or 2.5µg/ml Blasticidin (Sigma) and 20µM TMP (Sigma)
792 for the control. Parasitemia was monitored using a flow cytometer, either a CyAn ADP
793 (Beckman Coulter) or CytoFLEX (Beckman Coulter) instrument, using either 1.5µg/ml
794 acridine orange (Molecular Probes) as described previously[35] or similarly using 8µM
795 Hoechst in filtered 1X phosphate-buffered saline (PBS). Flow cytometry data were

796 analyzed using FlowJo software (Treestar Inc.). If the parasitemia was too high, parasites
797 were subcultured during the experiment and the relative parasitemia was then calculated
798 by multiplying the calculated parasitemia by the dilution factor. Parasitemia was
799 normalized by using the highest parasitemia as one hundred percent. Using Prism
800 software (GraphPad Software Inc), the parasitemia data were fit to an exponential growth
801 curve equation.
802
803 To determine the EC_{50} of TMP for PfGRP170-GFP-DDD cell lines, parasites were washed
804 as described above and seeded into a 96 well plate with 2.5µg/ml Blasticidin and varying
805 TMP concentrations. Parasitemia was measured after 48 hours using flow cytometry as
806 described above. The parasitemia data were fit to a dose-response equation using Prism.
807 For the IPP rescue experiment, asynchronous PfGRP170-GFP-DDD parasites were
808 washed as described above and resuspended in media either with 2.5µg/ml Blasticidin or
809 2.5µg/ml Blasticidin and 20µM TMP with or without 200µM Isopentenyl pyrophosphate
810 (Isoprenoids LC). Parasitemia were monitored using flow cytometry as described above
811 and the data were fit to an exponential growth curve equation using Prism.
812
813 For the heat shock experiment, asynchronous PfGRP170-GFP-DDD parasites were
814 washed as described above and resuspended in media either with 2.5µg/ml Blasticidin or
815 2.5µg/ml Blasticidin and 20µM TMP. Parasites were then incubated at either 37°C or 40°C
816 for 6 hours. After 6 hours, 20µM TMP was added to cultures that were incubated without
817 it and all parasites were shifted back to 37ºC. Parasitemia was monitored using flow
818 cytometry as described above and the data were fit to an exponential growth curve
819 equation (GraphPad Software Inc).
820
821 For growth assays done with PfGRP170-GFP-DDD-GFP cell lines overexpressing PfBiP,
822 asynchronous parasites were washed as described above and resuspended in media
823 either with 2.5µg/ml Blasticidin and 250nM of DSM1 or 2.5µg/ml Blasticidin, 250nM of
824 DSM1, and 20µM TMP. Parasitemia were monitored using flow cytometry as described
825 above and the data were fit to an exponential growth curve equation using Prism.
826

827 ***Synchronized growth assay***

828 PfGRP170-GFP-DDD Parasites were synchronized as described previously by sorbitol
829 (VWR), followed by percoll (Genesee Scientific) the next day and then sorbitol four hours
830 later to obtain 0-4 hour rings[32,36]. Parasites were washed as described above to remove
831 TMP from the media and incubated in media either with 2.5µg/ml Blasticidin or 2.5µg/ml
832 Blasticidin and 20µM TMP. Thin blood smears using the Hema 3 Staining Kit
833 (PROTOCOL/Fisher) were prepared every few hours to monitor parasite growth and
834 morphology. Slides were imaged using a Nikon Eclipse E400 microscope with a Nikon
835 DS-L1-5M imaging camera.

836

837 ***Western blot***

838 Western blotting was performed as described previously[32]. Parasite pellets were isolated
839 using cold 0.04% Saponin (Sigma) in 1X PBS for 10 minutes as described previously[32,36].
840 Antibodies used for this study were: mouse anti-GFP JL-8 (Clontech, 1:3000), rabbit anti-
841 PfEF1α (from D. Goldberg, 1:2,000), mouse anti-plasmepsin V (from D. Goldberg, 1:400),
842 rabbit anti-PfBiP MRA-1246 (BEI resources, 1:500), rabbit anti-GFP A-6455 (Invitrogen,
843 1:2,000), mouse anti-eIF2α L57A5 (Cell Signaling, 1:1,000), rabbit anti- Phospho-eIF2α
844 119A11 (Cell Signaling, 1:1,000), rat anti-HA (Roche 3F10, 1:3000), mouse anti-Ty1
845 (Sigma Clone BB2, 1:1000), and mouse anti-Ub P4D1 (Santa Cruz Biotechnology,
846 1:1,000). Secondary antibodies used were IRDye 680CW goat anti-rabbit IgG and IRDye
847 800CW goat anti-mouse IgG (LICOR Biosciences, 1:20,000). The western blots were
848 imaged using the Odyssey infrared imaging system. Polyacrylamide gels used in this
849 study were either prepared using 10% EZ-Run protein gel solution (Fisher) or precast
850 gradient gels (4-20%, from Biorad). Any quantification performed on western blots was
851 done using ImageJ software. The quantification data were analyzed using Prism
852 (GraphPad Software, Inc.).

853

854

855 ***PK4 Inhibitor Experiments***

856 Synchronized ring stage PfGRP170-GFP-DDD parasites were incubated in media with
857 either 2.5µg/ml Blasticidin or 2.5µg/ml Blasticidin and 20µM TMP in the presence or

858 absence of a PK4 inhibitor GSK2606414 (Millipore Sigma) at 2μM for 24 hours. After 24
859 hours, the parasites were lysed for western blot analysis using 0.04% saponin in 1X PBS
860 as described above. PM1 (parental control parasites) were incubated in media with either
861 complete RPM1 (no drug) or media containing 20μM TMP in the presence or absence of
862 PK4 inhibitor GSK2606414 (Millipore Sigma) at 2μM for 24 hours. After 24 hours, the
863 parasites were lysed for western blot analysis using 0.04% saponin in 1X PBS as
864 described above.
865
866 ***Live Fluorescence Microscopy***
867 To visualize PfGRP170-GFP-DDD live parasites, 100μL of parasite culture was pelleted.
868 The supernatant was removed, and the parasites were resuspended in 100μL medium
869 with 2.5μg/ml Blasticidin and 20μM TMP and 5μM Hoechst. The parasites were incubated
870 at 37°C for 20 minutes. The parasites were then pelleted again and 90% of the medium
871 was removed. Parasites were resuspended in the remaining medium and 8μL of this
872 culture was placed on a glass slide and covered with a coverslip. The edges were sealed
873 with nail polish and the cells were imaged using a DeltaVision II Microscope.
874
875 ***Immunofluorescence trafficking assays and imaging processing***
876 Immunofluorescence assays (IFA) were performed as described previously using a
877 combination of 4% Paraformaldehyde and 0.015% glutaraldehyde for fixation and
878 permeabilization using 0.1% Triton-X100[32,35] or by smearing cells on a slide and fixing
879 them with acetone. For apicoplast and red blood cell trafficking assays, cells were
880 synchronized and TMP was removed as described above. Cells were then fixed as
881 described above, 24 hours after the removal of TMP.
882
883 Primary antibodies used for IFAs in this study were: rabbit anti-GFP A-6455 (Invitrogen,
884 1:200), rat anti-PfBiP MRA-1247 (BEI resources, 1:125), rabbit anti-PfBiP MRA-1246 (BEI
885 resources (1:100), mouse anti-plasmepsin V (From D. Goldberg, 1:1), mouse anti-GFP
886 clones 7.1 and 13.1 (Roche 11814460001, 1:500), rabbit anti-Cpn60 (From. B. Striepen,
887 1:1,000), rabbit anti-PfERD2 (MR4, 1:2,000), rabbit anti-HA 9110 (Abcam, 1:200), rabbit
888 anti-PfMAHRP1C (From. Hans-Peter Beck, 1:500), mouse anti-PfFIKK4.2 (From David

889 Cavanagh/EMRR, 1:1,000), mouse anti-Ty1 (Sigma Clone BB2, 1:200), and rabbit anti-
890 PfHSP70X (From Jude Przyborski, 1:500). Secondary antibodies used in this study are
891 Alexa Fluor goat anti-rabbit 488, Alexa Fluor goat anti-rabbit 546, Alexa Fluor goat anti-
892 mouse 488, Alexa Fluor goat anti-mouse 546, and Alexa Fluor goat anti-rat 546 (Life
893 Technologies, 1:100). The mouse anti-PfFIKK4.2, rabbit anti-PfHSP70X, and anti-
894 PfMAHRP1C require acetone fixation.
895
896 All fixed cells were mounted using ProLong Diamond with DAPI (Invitrogen) and imaged
897 using the DeltaVision II microscope system or Zeiss ELYRA S1 (SR-SIM) Super
898 Resolution Microscope using a 100X objective. Images taken using the DeltaVision II
899 were collected as a Z-stack and were deconvolved using the DeltaVision II software
900 (SoftWorx). The deconvolved Z-stacks were then displayed as a maximum intensity
901 projection using SoftWorx. Images taken using the Super Resolution Microscope were
902 taken as a Z-stack. The Z-stacks were analyzed using Zen Software (Zeiss, version from
903 2011) for SIM processing and obtaining the maximum intensity projection. Any
904 adjustments made to the brightness and/or contrast of the images were made using either
905 Softworx, Zen Software, or Adobe Photoshop and were done for display purposes only.
906 Any quantification performed for microscopy images was done using ImageJ software as
907 described previously[35]. The quantification data were analyzed using Prism (GraphPad
908 Software, Inc.).
909 ***Co-immunoprecipitation assays and Mass Spectroscopy***
910 Parasites pellets were isolated from 48 mL of asynchronous culture at high parasitemia
911 (10% or higher) using cold 0.04% saponin in 1X PBS as described above. Parasite pellets
912 were lysed by resuspending the pellet in 150µL of Extraction Buffer (40mM Tris HCL pH
913 7.6, 150mM KCL, and 1mM EDTA) with 0.5% NP-40 (VWR) and 1X HALT protease
914 inhibitor (Thermo). The resuspended parasites were then incubated on ice for 15 minutes
915 and then sonicated three times (10% amplitude, 5 second pulses). In between each
916 sonication, the lysate was placed on ice for 1 minute. The lysate was then centrifuged at
917 21,100g for 15 minutes at 4ºC. The supernatant was collected in a fresh tube and placed
918 on ice. The remaining pellet was subjected to a second lysis step using 150µL of
919 Extraction buffer as above without NP-40. The lysate was sonicated and centrifuged as

920 above (no 15-minute incubation on ice). The supernatant was collected and combined
921 with the lysate from the first lysis step (INPUT sample). 20µL of the input sample was
922 collected into a fresh tube and stored in the -80ºC. The remaining input sample was
923 combined with 2µL of rabbit anti-GFP monoclonal G10362 (Thermo) and incubated
924 rocking for two hours at 4°C.
925
926 After the two-hour incubation, the lysate with antibody was added to 50µL of prepared
927 protein G Dynabeads (Invitrogen). Dynabeads were prepared by washing 50µL of beads
928 three times with 100µL of IgG binding buffer (20mM Tris HCL pH 7.6, 150mM KCL, 1mM
929 EDTA, and 0.1% NP-40). The IgG binding buffer was removed from the beads each time
930 using a magnetic rack (Life technologies). The beads, antibody, and lysate were
931 incubated rocking for two hours at 4°C. After the two-hour incubation, the unbound
932 fraction of protein was collected using the magnetic rack into a fresh tube and stored at -
933 80°C until needed for western blot analysis. The beads were then washed two times in
934 300µL of IgG binding buffer with 1X HALT and one time in IgG binding buffer with 1X
935 HALT without NP-40. Each wash was done for 10 minutes rocking at 4°C.
936
937 For Co-IP's to show PfGRP170-GFP-DDD/BiP interaction 0-4 hour ring stage parasites
938 were obtained and TMP was removed as described under the synchronized growth assay
939 section. Parasites were lysed and an anti-GFP IP was performed as described above,
940 approximately 24 hours after the removal of TMP. Protein was eluted off the beads for
941 western blot using 1X Protein Loading Dye (LICOR) with 2.5% beta-Mercaptoethanol
942 (Fisher) and boiled for 5 minutes. This was followed by a centrifugation at 16,200 g for 5
943 minutes. The eluted proteins are collected by placing the tube on a magnetic rack. The
944 isolated proteins on magnetic beads were digested with trypsin and analyzed at the
945 Emory University Integrated Proteomics Core using a Fusion Orbitrap Mass
946 Spectrometer.
947
948 ***PfGRP170-BirA biotinylation and mass spectrometry***
949 To confirm that proteins were biotinylated when biotin was added to the PfGRP170-BirA
950 parasites, parasites were incubated 24 hours in media containing 2.5nM WR + 150µg of

951 biotin (Sigma). Parasites were isolated using 0.04% saponin in 1X PBS and the lysates
952 were analyzed via western blot as described above. Secondary antibodies used were
953 IRDye 680CW goat anti-rabbit IgG and IRDye 800CW Streptavidin (LICOR). 3D7
954 parasites incubated with media containing 150µg of biotin for 24 hours was used as a
955 control.
956
957 For PfGRP170-HA-BirA streptavidin IP's, cultures were incubated for 24 hours in media
958 containing 2.5nM WR + 150µg of biotin (Sigma). 48 mL of asynchronous culture at high
959 parasitemia (10% or higher) were harvested for IP as described above with the following
960 modifications. Streptavidin MagneSphere Paramagnetic Particle beads (Promega) were
961 used to isolated biotinylated proteins. To prepare the Streptavidin beads for IP, beads
962 were washed three times in 1 mL of 1X PBS. Incubations of lysate with the magnetic
963 beads were performed at room temperature for 30 minutes. After the unbound fraction
964 was removed, beads were washed twice in 8M Urea (150mM NaCL, 50mM Tris HCL pH
965 7.4) and once in 1X PBS. The biotinylated proteins on magnetic beads were digested with
966 trypsin and analyzed at the Emory University Integrated Proteomics Core using a Fusion
967 Orbitrap Mass Spectrometer. 3D7 control streptavidin IP's were conducted as above but
968 without the addition of 2.5nM WR to the media.
969
970 ***Proximity Ligation Assays***
971 Asynchronous PfGRP170-GFP-DDD parasites were fixed as described above,
972 approximately 24 hours after the removal of TMP. The proximity ligation assay was
973 performed using the Duolink PLA Fluorescence kit (Sigma) per the manufacturers
974 protocol. For the BiP/PfGRP170 PLA assay, primary antibodies mouse anti-GFP (Roche
975 11814460001, 1:500) and rabbit anti-BiP MRA-1246 (BEI resources (1:100) were used.
976 For the negative control primary antibodies mouse anti-plasmepsin V (From D. Goldberg,
977 1:1) and rabbit anti-GFP A-6455 (Invitrogen, 1:200) were used.
978
979 ***Ring Stage Survival Assay***
980 The ring-stage survival assay method was performed on 3D7 (control) and PfGRP170-
981 BirA parasites as described previously, with a slight adjustment[80]. Cultures were

982 synchronized using 5% sorbitol (Sigma-Aldrich, St. Louis, MO, USA), pre-warmed to
983 37°C, to obtain the highest proportion of rings, ≥50%. The cultures were placed back
984 under previously described conditions for 24 hours and followed-up the next morning.
985 Thin blood smears were methanol fixed and stained with 10% Giemsa for 15 minutes and
986 evaluated for mature schizonts with visible nuclei (10-12). The parasites were
987 independently suspended in PRMI-1640 supplemented with 15U/ml of sodium heparin
988 (Sigma-Aldrich, St. Louis, MO, USA) to disrupt spontaneous rosettes formation for 15
989 minutes at 37 °C. After incubation, each parasite culture was layered onto a 75/25%
990 percoll (GE Healthcare Life Sciences, Pittsburgh, PA, USA) gradient, and centrifuged at
991 3000rpm for 15 minutes. The intermediate phases containing the mature schizonts of
992 each culture, were independently collected, gently washed in RPMI and transferred into
993 two new T25 flasks with fresh cRPMI and erythrocytes for 3-hour incubation at previously
994 described conditions. Thin blood smears were prepared as previously described, to
995 ensure >10% schizonts count.
996
997 At the 3-hour mark, the parasites were taken-out of incubation and treated with 5%
998 sorbitol to remove the remaining mature schizonts, which had not invaded erythrocytes
999 yet. Parasitemia was adjusted to 1% at 2% hematocrit by adding uninfected erythrocytes
1000 and cPRMI, after the evaluation of quick stained Giemsa smears. The parasites were
1001 exposed to 700nM DHA or 1% dimethyl sulfoxide (DMSO) for 6 hours. After the 6-hour
1002 incubation period, the parasites were washed to remove the drug or DMSO and re-
1003 suspended in 1ml of cRPMI. The parasites were then transferred into two new well in the
1004 48-well culture plate, incubated at 37 °C under a 90 % N_2, 5 % CO_2, and 5 % O_2 gas
1005 mixture for 66 hours, after which thin blood smears were prepared, methanol fixed,
1006 stained with 10% Giemsa for 15 minutes and read by three operators. Growth rate and
1007 percent survival was calculated by counting the number of parasitized cells in an
1008 estimated 2000 erythrocytes.
1009
1010 **REFERENCES**
1011 1 World Health Organization. World Malaria Report. (2017).

1012 2 Amaratunga, C., Witkowski, B., Khim, N., Menard, D. & Fairhurst, R. M.
1013 Artemisinin resistance in Plasmodium falciparum. *The Lancet Infectious Disease*
1014 **14**, 449-450 (2014).
1015 3 Dondorp, A. M. *et al.* Artemisinin resistance in Plasmodium falciparum malaria. *N*
1016 *Engl J Med* **361**, 455-467, doi:10.1056/NEJMoa0808859 (2009).
1017 4 Roper, C. *et al.* Intercontinental spread of pyrimethamine-resistant malaria.
1018 *Science* **305**, 1124 (2004).
1019 5 Wootton, J. C. *et al.* Genetic diversity and chloroquine selective sweeps in
1020 Plasmodium falciparum. *Nature* **418**, 320-323 (2002).
1021 6 Mita, T. *et al.* Limited geographical origin and global spread of sulfadoxine-
1022 resistant dhps alleles in Plasmodium falciparum populations. *J Infect Dis* **204**,
1023 1980-1988, doi:10.1093/infdis/jir664 (2011).
1024 7 Miller, L. H., Baruch, D. I., Marsh, K. & Doumbo, O. K. The pathogenic basis of
1025 malaria. *Nature* **415**, 673-679 (2002).
1026 8 Mok, S. *et al.* Drug resistance. Population transcriptomics of human malaria
1027 parasites reveals the mechanism of artemisinin resistance. *Science* **347**, 431-
1028 435, doi:10.1126/science.1260403 (2015).
1029 9 Rocamora, F. *et al.* Oxidative stress and protein damage responses mediate
1030 artemisinin resistance in malaria parasites. *PLoS Pathog* **14**, e1006930,
1031 doi:10.1371/journal.ppat.1006930 (2018).
1032 10 Zhang, M. *et al.* Inhibiting the Plasmodium eIF2alpha Kinase PK4 Prevents
1033 Artemisinin-Induced Latency. *Cell Host Microbe* **22**, 766-776 e764,
1034 doi:10.1016/j.chom.2017.11.005 (2017).
1035 11 Deponte, M. *et al.* Wherever I may roam: protein and membrane trafficking in P.
1036 falciparum-infected red blood cells. *Mol Biochem Parasitol* **186**, 95-116,
1037 doi:10.1016/j.molbiopara.2012.09.007 (2012).
1038 12 Boddey, J. A. & Cowman, A. F. Plasmodium nesting: remaking the erythrocyte
1039 from the inside out. *Annu Rev Microbiol* **67**, 243-269, doi:10.1146/annurev-micro-
1040 092412-155730 (2013).
1041 13 Boddey, J. A. *et al.* Role of plasmepsin V in export of diverse protein families
1042 from the Plasmodium falciparum exportome. *Traffic* **14**, 532-550,
1043 doi:10.1111/tra.12053 (2013).
1044 14 Russo, I. *et al.* Plasmepsin V licenses Plasmodium proteins for export into the
1045 host erythrocyte. *Nature* **463**, 632-636, doi:10.1038/nature08726 (2010).
1046 15 Tonkin, C. J., Kalanon, M. & McFadden, G. I. Protein targeting to the malaria
1047 parasite plastid. *Traffic* **9**, 166-175, doi:10.1111/j.1600-0854.2007.00660.x
1048 (2008).
1049 16 Zhang, M. *et al.* PK4, a eukaryotic initiation factor 2α(eIF2α) kinase, is essential
1050 for the development of the erythrocytic cycle of Plasmodium. *PNAS* **109**, 3956–
1051 3961 (2012).
1052 17 Walter, P. & David, R. The unfolded protein response: from stress pathway to
1053 homeostatic regulation. *Science* **334**, 1081-1086 (2011).
1054 18 Araki, K. & Nagata, K. Protein folding and quality control in the ER. *Cold Spring*
1055 *Harb Perspect Biol* **3**, a007526, doi:10.1101/cshperspect.a007526 (2011).

1056 19 Gidalevitz, T., Stevens, F. & Argon, Y. Orchestration of secretory protein folding
1057 by ER chaperones. *Biochim Biophys Acta* **1833**, 2410-2424,
1058 doi:10.1016/j.bbamcr.2013.03.007 (2013).
1059 20 Hotamisligil, G. S. Endoplasmic reticulum stress and atherosclerosis. *Nat Med*
1060 **16**, 396-399, doi:10.1038/nm0410-396 (2010).
1061 21 Xu, C., Bailly-Maitre, B. & Reed, J. C. Endoplasmic reticulum stress: cell life and
1062 death decisions. *J Clin Invest* **115**, 2656-2664, doi:10.1172/JCI26373 (2005).
1063 22 Rutkowski, D. T. & Hegde, R. S. Regulation of basal cellular physiology by the
1064 homeostatic unfolded protein response. *J Cell Biol* **189**, 783-794,
1065 doi:10.1083/jcb.201003138 (2010).
1066 23 Wang, H. *et al.* The Endoplasmic Reticulum Chaperone GRP170: From
1067 Immunobiology to Cancer Therapeutics. *Front Oncol* **4**, 377,
1068 doi:10.3389/fonc.2014.00377 (2014).
1069 24 Pavithra, S. R., Kumar, R. & Tatu, U. Systems analysis of chaperone networks in
1070 the malarial parasite Plasmodium falciparum. *PLoS Comput Biol* **3**, 1701-1715,
1071 doi:10.1371/journal.pcbi.0030168 (2007).
1072 25 Shonhai, A., Boshoff, A. & Blatch, G. L. The structural and functional diversity of
1073 Hsp70 proteins from Plasmodium falciparum. *Protein Sci* **16**, 1803-1818,
1074 doi:10.1110/ps.072918107 (2007).
1075 26 Andreasson, C., Rampelt, H., Fiaux, J., Druffel-Augustin, S. & Bukau, B. The
1076 endoplasmic reticulum Grp170 acts as a nucleotide exchange factor of Hsp70 via
1077 a mechanism similar to that of the cytosolic Hsp110. *J Biol Chem* **285**, 12445-
1078 12453, doi:10.1074/jbc.M109.096735 (2010).
1079 27 de Keyzer, J., Steel, G. J., Hale, S. J., Humphries, D. & Stirling, C. J. Nucleotide
1080 binding by Lhs1p is essential for its nucleotide exchange activity and for function
1081 in vivo. *J Biol Chem* **284**, 31564-31571, doi:10.1074/jbc.M109.055160 (2009).
1082 28 Behnke, J. & Hendershot, L. M. The large Hsp70 Grp170 binds to unfolded
1083 protein substrates in vivo with a regulation distinct from conventional Hsp70s. *J*
1084 *Biol Chem* **289**, 2899-2907, doi:10.1074/jbc.M113.507491 (2014).
1085 29 Park, J. *et al.* The Chaperoning Properties of Mouse Grp170, a Member of the
1086 Third Family of Hsp70 Related Proteins. *Biochemistry* **42**, 14893-14902 (2003).
1087 30 Buck, T. M. *et al.* The Lhs1/GRP170 chaperones facilitate the endoplasmic
1088 reticulum-associated degradation of the epithelial sodium channel. *J Biol Chem*
1089 **288**, 18366-18380, doi:10.1074/jbc.M113.469882 (2013).
1090 31 Beck, J. R., Muralidharan, V., Oksman, A. & Goldberg, D. E. PTEX component
1091 HSP101 mediates export of diverse malaria effectors into host erythrocytes.
1092 *Nature* **511**, 592-595, doi:10.1038/nature13574 (2014).
1093 32 Florentin, A. *et al.* PfClpC Is an Essential Clp Chaperone Required for Plastid
1094 Integrity and Clp Protease Stability in Plasmodium falciparum. *Cell Rep* **21**, 1746-
1095 1756, doi:10.1016/j.celrep.2017.10.081 (2017).
1096 33 Muralidharan, V., Oksman, A., Pal, P., Lindquist, S. & Goldberg, D. E.
1097 Plasmodium falciparum heat shock protein 110 stabilizes the asparagine repeat-
1098 rich parasite proteome during malarial fevers. *Nat Commun* **3**, 1310-1310 (2012).
1099 34 Easton, D. P., Kaneko, Y. & Subjeck, J. R. The hsp110 and Grp170 stress
1100 proteins: newly recognized relatives of the Hsp70s. *Cell Stress Chaperones* **5**,
1101 276-290 (2000).

1102 35 Cobb, D. W. *et al.* The Exported Chaperone PfHsp70x Is Dispensable for the
1103 Plasmodium falciparum Intraerythrocytic Life Cycle. *mSphere* **2**,
1104 doi:10.1128/mSphere.00363-17 (2017).
1105 36 Muralidharan, V., Oksman, A., Iwamoto, M., Wandless, T. J. & Goldberg, D. E.
1106 Asparagine repeat function in a Plasmodium falciparum protein assessed via a
1107 regulatable fluorescent affinity tag. *Proc Natl Acad Sci U S A* **108**, 4411-4416,
1108 doi:10.1073/pnas.1018449108 (2011).
1109 37 Ganter, M. *et al.* Plasmodium falciparum CRK4 directs continuous rounds of DNA
1110 replication during schizogony. *Nat Microbiol* **2**, 17017,
1111 doi:10.1038/nmicrobiol.2017.17 (2017).
1112 38 Ito, D., Schureck, M. A. & Desai, S. A. An essential dual-function complex
1113 mediates erythrocyte invasion and channel-mediated nutrient uptake in malaria
1114 parasites. *Elife* **6**, doi:10.7554/eLife.23485 (2017).
1115 39 Waller, R. F., Reed, M. B., Cowman, A. F. & McFadden, G. I. Protein trafficking
1116 to the plastid of Plasmodium falciparum is via the secretory pathway. *EMBO J*
1117 **19**, 1794-1802 (2000).
1118 40 Tonkin, C. J., Struck, N. S., Mullin, K. A., Stimmler, L. M. & McFadden, G. I.
1119 Evidence for Golgi-independent transport from the early secretory pathway to the
1120 plastid in malaria parasites. *Mol Microbiol* **61**, 614-630, doi:10.1111/j.1365-
1121 2958.2006.05244.x (2006).
1122 41 Heiny, S. R., Pautz, S., Recker, M. & Przyborski, J. M. Protein Traffic to the
1123 Plasmodium falciparum apicoplast: evidence for a sorting branch point at the
1124 Golgi. *Traffic* **15**, 1290-1304, doi:10.1111/tra.12226 (2014).
1125 42 Fellows, J. D., Cipriano, M. J., Agrawal, S. & Striepen, B. A Plastid Protein That
1126 Evolved from Ubiquitin and Is Required for Apicoplast Protein Import in
1127 Toxoplasma gondii. *mBio* **8**, 1-18 (2017).
1128 43 Sheiner, L. *et al.* A systematic screen to discover and analyze apicoplast proteins
1129 identifies a conserved and essential protein import factor. *PLoS Pathog* **7**,
1130 e1002392, doi:10.1371/journal.ppat.1002392 (2011).
1131 44 Yeh, E. & DeRisi, J. L. Chemical rescue of malaria parasites lacking an
1132 apicoplast defines organelle function in blood-stage Plasmodium falciparum.
1133 *PLoS Biol* **9**, e1001138, doi:10.1371/journal.pbio.1001138 (2011).
1134 45 Chen, A. L. *et al.* Novel components of the Toxoplasma inner membrane
1135 complex revealed by BioID. *MBio* **6**, e02357-02314, doi:10.1128/mBio.02357-14
1136 (2015).
1137 46 Painter, H. J. *et al.* Genome-wide real-time in vivo transcriptional dynamics
1138 during Plasmodium falciparum blood-stage development. *Nat Commun* **9**, 2656,
1139 doi:10.1038/s41467-018-04966-3 (2018).
1140 47 Soderberg, O. *et al.* Direct observation of individual endogenous protein
1141 complexes in situ by proximity ligation. *Nat Methods* **3**, 995-1000,
1142 doi:10.1038/nmeth947 (2006).
1143 48 Gullberg, M. *et al.* Cytokine detection by antibody-based proximity ligation. *Proc*
1144 *Natl Acad Sci U S A* **101**, 8420-8424, doi:10.1073/pnas.0400552101 (2004).
1145 49 Fredriksson, S. *et al.* Protein detection using proximity-dependent DNA ligation
1146 assays. *Nature Biotechnology* **20**, 473-477 (2002).

1147 50 Kulzer, S. *et al.* Plasmodium falciparum-encoded exported hsp70/hsp40
1148 chaperone/co-chaperone complexes within the host erythrocyte. *Cell Microbiol*
1149 **14**, 1784-1795, doi:10.1111/j.1462-5822.2012.01840.x (2012).
1150 51 Tyson, J. R. & Stirling, C. J. LHS1 and SIL1 provide a lumenal function that is
1151 essential for protein translocation into the endoplasmic reticulum. *The EMBO*
1152 *Journal* **19**, 6440-6452 (2000).
1153 52 Harbut, M. B. *et al.* Targeting the ERAD pathway via inhibition of signal peptide
1154 peptidase for antiparasitic therapeutic design. *Proc Natl Acad Sci U S A* **109**,
1155 21486-21491 (2012).
1156 53 Chaubey, S., Grover, M. & Tatu, U. Endoplasmic reticulum stress triggers
1157 gametocytogenesis in the malaria parasite. *J Biol Chem* **289**, 16662-16674,
1158 doi:10.1074/jbc.M114.551549 (2014).
1159 54 Fennell, C. *et al.* PfeIK1, a eukaryotic initiation factor 2alpha kinase of the human
1160 malaria parasite Plasmodium falciparum, regulates stress-response to amino-
1161 acid starvation. *Malar J* **8**, 99, doi:10.1186/1475-2875-8-99 (2009).
1162 55 Babbitt, S. E. *et al.* Plasmodium falciparum responds to amino acid starvation by
1163 entering into a hibernatory state. *Proc Natl Acad Sci U S A* **109**, E3278-3287
1164 (2012).
1165 56 Ward, P., Equinet, L., Packer, J. & Doerig, C. Protein kinases of the human
1166 malaria parasite Plasmodium falciparum: the kinome of a divergent eukaryote.
1167 *BMC Genomics* **5**, 79, doi:10.1186/1471-2164-5-79 (2004).
1168 57 Foth, B. J. *et al.* Dissecting Apicoplast Targeting in the Malaria Parasite
1169 Plasmodium falciparum. *Science* **299**, 705-708 (2003).
1170 58 Ramya, T. N., Karmodiya, K., Surolia, A. & Surolia, N. 15-deoxyspergualin
1171 primarily targets the trafficking of apicoplast proteins in Plasmodium falciparum. *J*
1172 *Biol Chem* **282**, 6388-6397, doi:10.1074/jbc.M610251200 (2007).
1173 59 Ramya, T. N., Surolia, N. & Surolia, A. 15-Deoxyspergualin modulates
1174 Plasmodium falciparum heat shock protein function. *Biochem Biophys Res*
1175 *Commun* **348**, 585-592, doi:10.1016/j.bbrc.2006.07.082 (2006).
1176 60 Gruring, C. *et al.* Uncovering common principles in protein export of malaria
1177 parasites. *Cell Host Microbe* **12**, 717-729, doi:10.1016/j.chom.2012.09.010
1178 (2012).
1179 61 Boddey, J. A. *et al.* Export of malaria proteins requires co-translational
1180 processing of the PEXEL motif independent of phosphatidylinositol-3-phosphate
1181 binding. *Nat Commun* **7**, 10470, doi:10.1038/ncomms10470 (2016).
1182 62 Marti, M., Good, R. T., Rug, M., Knuepfer, E. & Cowman, A. F. Targeting malaria
1183 virulence and remodeling proteins to the host erythrocyte. *Science* **306**, 1930-
1184 1933 (2004).
1185 63 Hiller, N. L. *et al.* A Host-Targeting Signal in Virulence Proteins Reveals a
1186 Secretome in Malarial Infection. *Science* **306** (2015).
1187 64 Heiny, S. R., Spork, S. & Przyborski, J. The apicoplast of the human malaria
1188 parasite P. falciparum. *Journal of Endocytobiosis and Cell Research* **23**, 91-95
1189 (2012).
1190 65 Batinovic, S. *et al.* An exported protein-interacting complex involved in the
1191 trafficking of virulence determinants in Plasmodium-infected erythrocytes. *Nat*
1192 *Commun* **8**, 16044, doi:10.1038/ncomms16044 (2017).

1193 66 Wang, Y. *et al.* Involvement of oxygen-regulated protein 150 in AMP-activated
1194 protein kinase-mediated alleviation of lipid-induced endoplasmic reticulum stress.
1195 *J Biol Chem* **286**, 11119-11131, doi:10.1074/jbc.M110.203323 (2011).
1196 67 Sanson, M. *et al.* Oxidized low-density lipoproteins trigger endoplasmic reticulum
1197 stress in vascular cells: prevention by oxygen-regulated protein 150 expression.
1198 *Circ Res* **104**, 328-336, doi:10.1161/CIRCRESAHA.108.183749 (2009).
1199 68 Yoshida, H., Matsui, T., Yamamoto, A., Okada, T. & Mori, K. XBP1 mRNA Is
1200 Induced by ATF6 and Spliced by IRE1 in Response to ER Stress to Produce a
1201 Highly Active Transcription Factor. *Cell* **107**, 881-891,
1202 doi:https://doi.org/10.1016/S0092-8674(01)00611-0 (2001).
1203 69 Collins, C. R., Hackett, F., Atid, J., Tan, M. S. Y. & Blackman, M. J. The
1204 Plasmodium falciparum pseudoprotease SERA5 regulates the kinetics and
1205 efficiency of malaria parasite egress from host erythrocytes. *PLoS Pathog* **13**,
1206 e1006453, doi:10.1371/journal.ppat.1006453 (2017).
1207 70 Ruecker, A. *et al.* Proteolytic activation of the essential parasitophorous vacuole
1208 cysteine protease SERA6 accompanies malaria parasite egress from its host
1209 erythrocyte. *J Biol Chem* **287**, 37949-37963, doi:10.1074/jbc.M112.400820
1210 (2012).
1211 71 Thomas, J. A. *et al.* A protease cascade regulates release of the human malaria
1212 parasite Plasmodium falciparum from host red blood cells. *Nat Microbiol* **3**, 447-
1213 455, doi:10.1038/s41564-018-0111-0 (2018).
1214 72 Zhao, X. *et al.* PfRON3 is an erythrocyte-binding protein and a potential blood-
1215 stage vaccine candidate antigen. *Malaria Journal* **13**, 490, doi:10.1186/1475-
1216 2875-13-490 (2014).
1217 73 Ling, I. T. *et al.* The Plasmodium falciparum clag9 gene encodes a rhoptry
1218 protein that is transferred to the host erythrocyte upon invasion. *Mol Microbiol* **52**,
1219 107-118, doi:10.1111/j.1365-2958.2003.03969.x (2004).
1220 74 Trenholme, K. R. *et al.* clag9: A cytoadherence gene in Plasmodium falciparum
1221 essential for binding of parasitized erythrocytes to CD36. *Proceedings of the*
1222 *National Academy of Sciences of the United States of America* **97**, 4029-4033,
1223 doi:10.1073/pnas.040561197 (2000).
1224 75 Balu, B., Shoue, D. A., Fraser, M. J., Jr. & Adams, J. H. High-efficiency
1225 transformation of Plasmodium falciparum by the lepidopteran transposable
1226 element piggyBac. *Proc Natl Acad Sci U S A* **102**, 16391-16396,
1227 doi:10.1073/pnas.0504679102 (2005).
1228 76 van Ooij, C. *et al.* The malaria secretome: from algorithms to essential function in
1229 blood stage infection. *PLoS Pathog* **4**, e1000084,
1230 doi:10.1371/journal.ppat.1000084 (2008).
1231 77 Li, M. Z. & Elledge, S. J. Harnessing homologous recombination in vitro to
1232 generate recombinant DNA via SLIC. *Nat Methods* **4**, 251-256,
1233 doi:10.1038/nmeth1010 (2007).
1234 78 Iwanaga, S., Kato, T., Kaneko, I. & Yuda, M. Centromere plasmid: a new genetic
1235 tool for the study of Plasmodium falciparum. *PLoS One* **7**, e33326,
1236 doi:10.1371/journal.pone.0033326 (2012).

1237 79 Ganesan, S. M. *et al.* Yeast dihydroorotate dehydrogenase as a new selectable
1238 marker for Plasmodium falciparum transfection. *Mol Biochem Parasitol* **177**, 29-
1239 34, doi:10.1016/j.molbiopara.2011.01.004 (2011).
1240 80 Witkowski, B. *et al.* Novel phenotypic assays for the detection of artemisinin-
1241 resistant Plasmodium falciparum malaria in Cambodia: in-vitro and ex-vivo drug-
1242 response studies. *The Lancet Infectious Diseases* **13**, 1043-1049,
1243 doi:10.1016/s1473-3099(13)70252-4 (2013).

1244